

# Analytical Template for the 4-Point Correlation Function Covariance Beyond the Gaussian Random Field I: 1-Loop Corrections involving Second-Order Densities

William Ortolá Leonard,<sup>1</sup> Zachary Slepian<sup>2</sup>

<sup>1</sup>Department of Physics, University of Florida,  
2001 Museum Rd., Gainesville, FL 32611, USA

<sup>2</sup>Department of Astronomy, University of Florida,  
211 Bryant Space Science Center, Gainesville, FL 32611, USA

E-mail: [wortola@ufl.edu](mailto:wortola@ufl.edu), [zslepian@ufl.edu](mailto:zslepian@ufl.edu)

**Abstract.** Analytical templates for the covariance matrix of the 4-Point Correlation Function (4PCF) have been developed in the past assuming a Gaussian Random Field (GRF). In this work, we present the first non-Gaussian calculation of the 4PCF covariance, incorporating 1-loop corrections using the second-order density contrast. Furthermore, we introduce a non-trivial galaxy bias scheme at second order. To simplify the calculation, we decompose the covariance into five distinct structures, and then exploit the isotropic basis functions of [3]. This approach reduces the complexity of the high-dimensional integrals naively involved, enabling the angular parts to be performed and leaving us with low-dimensional radial integrals. This analytical template will provide a more accurate characterization of the statistical errors on the 4PCF, improving both the parity-odd and parity-even analyses. This is the first paper in a two-part series.

---

## Contents

<b>1</b>	<b>Introduction</b>	<b>1</b>
<b>2</b>	<b>Setting Up the 1-Loop Covariance with Second-Order Densities</b>	<b>2</b>
<b>3</b>	<b>Modeling the 1-Loop Covariance with Second-Order Densities</b>	<b>6</b>
3.1	Fully-Connected Terms	7
3.1.1	Primary-Secondary Configuration	7
3.1.2	Half-Half Configuration	11
3.1.3	Primary-Primary Configuration	14
3.2	Partially-Connected Terms	15
3.2.1	PC-Primary-Secondary Configuration	17
3.2.2	PC-Half-Half Configuration	19
<b>4</b>	<b>Discussion and Conclusion</b>	<b>21</b>
<b>A</b>	<b>Generalizing the Second-Order Density Contrasts for Use in the Covariance Matrix</b>	<b>23</b>
A.1	Second-Order Density Kernel	23
A.2	Squared Linear Density Contrast	24
A.3	Tidal Tensor Kernel	24
A.4	Generalized Second-Order Density Contrast	25
<b>B</b>	<b>Evaluation of the Angular Integrals for the Covariance with Second-Order Densities</b>	<b>25</b>
<b>C</b>	<b>Evaluation of <math>\hat{s}</math> Integrals</b>	<b>27</b>
C.1	$\hat{s}$ Integral for the Primary-Secondary Configuration	27
C.2	$\hat{s}$ Integral for the Half-Half Configuration	29
C.3	$\hat{s}$ Integral for the Primary-Primary Configuration	29
C.4	$\hat{s}$ Integral for the PC-Primary-Secondary Configuration	30
C.5	$\hat{s}$ Integral for the PC-Half-Half Configuration	31
<b>D</b>	<b>Splitting Products of Mixed-Space 2-Argument Isotropic Basis Functions</b>	<b>32</b>
<b>E</b>	<b>Forming the Connected 4PCF Covariance</b>	<b>33</b>

---

## 1 Introduction

The Universe’s Large-Scale Structure (LSS) provides a unique laboratory for studying nature’s fundamental symmetries. A particular way to do this is by using the 4-Point Correlation Function (4PCF), incorporating a new tool to do cosmological inference and the possibility of detecting parity-odd modes. The connected, even- and odd-parity 4PCF have been measured using data from the Sloan Digital Sky Survey (SDSS) Baryon Oscillation Spectroscopic Survey (BOSS) by [9, 15, 16]; [9] reported the first measurement of parity-odd modes at  $7.1\sigma$ , followed by [16] with  $2.9\sigma$  evidence. Using data from Year 1 (Y1) of the Dark Energy Spectroscopic

Instrument (DESI), [10] measured the connected even-parity 4PCF, while [20], also found evidence of parity-violating signal between  $4\text{--}10\sigma$ . These searches were based on the method laid out in [4] and the basis of [3, 18], with the 4PCF covariance matrix from [8]. Although these results are statistically significant, it is imperative to confirm the robustness of this detection and evaluate it using more precise covariances.

Previous works have computed the matter [2, 12] and galaxy [21] power spectrum covariance matrices beyond the Gaussian Random Field (GRF). However, the 4PCF covariance matrix was modeled for the first time in [8] assuming a GRF density. While this treatment recovers the Gaussian (disconnected) covariance, it ignores the connected contributions from nonlinear mode coupling in the density field—effects that become non-negligible at  $k \gtrsim 0.1 [h \text{ Mpc}^{-1}]$ . In this work, we compute the next-to-leading-order contribution to the 4PCF covariance, incorporating nonlinear effects. To do so, we use Standard Perturbation Theory (SPT) modeling approach and include galaxy biasing up to second order. We compute the 4PCF covariance contributions from third-order densities in [14].

The structure of this work is as follows. In §2, we set up the next-to-leading-order covariance matrix, at tenth order in the linear density field using second-order density contrasts. In §3, we show how to mathematically model the covariance we previously set in §2. Then, we use the appendices to develop all the mathematical tools needed for §3.

## 2 Setting Up the 1-Loop Covariance with Second-Order Densities

The covariance is defined as [8]:

$$\text{Cov}(\zeta(\mathbf{R}), \zeta(\mathbf{R}')) \equiv \langle \zeta(\mathbf{R}) \zeta(\mathbf{R}') \rangle - \langle \zeta(\mathbf{R}) \rangle \langle \zeta(\mathbf{R}') \rangle, \quad (2.1)$$

where  $\zeta$  represents any N-Point Correlation Function (NPCF) we wish to evaluate and the angle bracket represents an average over realizations of the density field. We define  $\mathbf{R} \equiv (\mathbf{r}_0, \mathbf{r}_1, \dots, \mathbf{r}_{N-1})$ , and  $\mathbf{R}'$  in the same way. Following the procedure of [8], we evaluate the first term:

$$\langle \zeta(\mathbf{R}) \zeta(\mathbf{R}') \rangle = \int \frac{d^3 \mathbf{s}}{V} \left\langle \prod_{i=0}^{N-1} \delta_g(\mathbf{x} + \mathbf{r}_i) \delta_g(\mathbf{x} + \mathbf{r}'_i + \mathbf{s}) \right\rangle, \quad (2.2)$$

where the angle brackets represent the ensemble average of  $\mathbf{x}$ . We set  $N = 4$ , *i.e.*, we evaluate the 4PCF. Subscript “g” indicates the density fluctuations,  $\delta$ , are for galaxies, and  $V$  is the survey volume. Using the Eulerian bias expansion [1, 17]:

$$\delta_g(\mathbf{x}) = b_0 + b_1 \delta_m(\mathbf{x}) + \frac{b_2}{2} \delta_m^2(\mathbf{x}) + b_S S^{(2)}(\mathbf{x}),^1 \quad (2.3)$$

with  $b_0$  ensuring  $\langle \delta_g \rangle = 0$ , but will be omitted in the rest of this work since it does not enter connected correlation functions [17]. Then, the matter density contrast is expanded using SPT:

$$\delta_m(\mathbf{x}) = \delta_{\text{lin.}}(\mathbf{x}) + \delta^{(2)}(\mathbf{x}) + \mathcal{O}(\delta_{\text{lin.}}^3). \quad (2.4)$$

Above, we expanded the matter density contrast to second order in the linear density contrast,  $\delta_{\text{lin.}}$ ; we define  $\delta^{(2)}(\mathbf{x})$ ,  $\delta_{\text{lin.}}^2(\mathbf{x})$  and  $S^{(2)}(\mathbf{x})$  by their inverse Fourier Transforms in Appendix

---

<sup>1</sup>Other works may use  $b_2$  in place of our  $b_2/2$ , *e.g.* page 2 of [19].

A. We analyze the third-order terms in the second paper of the series [14]. Hence, inserting Eq. (2.4) into Eq. (2.3), and incorporating the resultant expression into Eq. (2.2), we obtain:

$$\begin{aligned} \langle \zeta(\mathbf{R}) \zeta(\mathbf{R}') \rangle = \int \frac{d^3 \mathbf{s}}{V} \left\langle \prod_{i=0}^3 \left[ b_1 \left( \delta_{\text{lin}} + \delta^{(2)} \right) + \frac{b_2}{2} \left( \delta_{\text{lin}} + \delta^{(2)} \right)^2 + b_S S^{(2)} \right] (\mathbf{x} + \mathbf{r}_i) \right. \\ \left. \times \left[ b_1 \left( \delta_{\text{lin}} + \delta^{(2)} \right) + \frac{b_2}{2} \left( \delta_{\text{lin}} + \delta^{(2)} \right)^2 + b_S S^{(2)} \right] (\mathbf{x} + \mathbf{r}'_i + \mathbf{s}) \right\rangle. \quad (2.5) \end{aligned}$$

Here, the arguments  $\mathbf{x} + \mathbf{r}_i$  and  $\mathbf{x} + \mathbf{r}'_i + \mathbf{s}$  apply to all terms inside the square brackets. Carrying out the product, we obtain the 1-loop covariance with second-order densities as:

$$\begin{aligned} \text{Cov}_{4,1\text{L}}^{[2]}(\mathbf{R}, \mathbf{R}') = & b_1^8 \left\{ \sum_{i=0}^3 \sum_{j=0}^3 \left\langle \delta^{(2)}(\mathbf{x} + \mathbf{r}_i) \delta^{(2)}(\mathbf{x} + \mathbf{r}'_j + \mathbf{s}) \right. \right. \\ & \times \prod_{p=0, p \neq i}^3 \prod_{t=0, t \neq j}^3 \delta_{\text{lin.}}(\mathbf{x} + \mathbf{r}_p) \delta_{\text{lin.}}(\mathbf{x} + \mathbf{r}'_t + \mathbf{s}) \left. \right\rangle \Big\} \\ & + b_1^6 \left( \frac{b_2}{2} \right)^2 \left\{ \sum_{i=0}^3 \sum_{j=0}^3 \left\langle \delta_{\text{lin.}}^2(\mathbf{x} + \mathbf{r}_i) \delta_{\text{lin.}}^2(\mathbf{x} + \mathbf{r}'_j + \mathbf{s}) \right. \right. \\ & \times \prod_{p=0, p \neq i}^3 \prod_{t=0, t \neq j}^3 \delta_{\text{lin.}}(\mathbf{x} + \mathbf{r}_p) \delta_{\text{lin.}}(\mathbf{x} + \mathbf{r}'_t + \mathbf{s}) \left. \right\rangle \Big\} \\ & + b_1^6 b_s^2 \left\{ \sum_{i=0}^3 \sum_{j=0}^3 \left\langle S^{(2)}(\mathbf{x} + \mathbf{r}_i) S^{(2)}(\mathbf{x} + \mathbf{r}'_j + \mathbf{s}) \right. \right. \\ & \times \prod_{p=0, p \neq i}^3 \prod_{t=0, t \neq j}^3 \delta_{\text{lin.}}(\mathbf{x} + \mathbf{r}_p) \delta_{\text{lin.}}(\mathbf{x} + \mathbf{r}'_t + \mathbf{s}) \left. \right\rangle \Big\} \\ & + b_1^7 \frac{b_2}{2} \left\{ \sum_{i=0}^3 \sum_{j=0}^3 \left\langle \delta_{\text{lin.}}^2(\mathbf{x} + \mathbf{r}_i) \delta^{(2)}(\mathbf{x} + \mathbf{r}'_j + \mathbf{s}) \right. \right. \\ & \times \prod_{p=0, p \neq i}^3 \prod_{t=0, t \neq j}^3 \delta_{\text{lin.}}(\mathbf{x} + \mathbf{r}_p) \delta_{\text{lin.}}(\mathbf{x} + \mathbf{r}'_t + \mathbf{s}) \left. \right\rangle + \text{symm.} \Big\} \\ & + b_1^6 b_s \frac{b_2}{2} \left\{ \sum_{i=0}^3 \sum_{j=0}^3 \left\langle \delta_{\text{lin.}}^2(\mathbf{x} + \mathbf{r}_i) S^{(2)}(\mathbf{x} + \mathbf{r}'_j + \mathbf{s}) \right. \right. \\ & \times \prod_{p=0, p \neq i}^3 \prod_{t=0, t \neq j}^3 \delta_{\text{lin.}}(\mathbf{x} + \mathbf{r}_p) \delta_{\text{lin.}}(\mathbf{x} + \mathbf{r}'_t + \mathbf{s}) \left. \right\rangle + \text{symm.} \Big\} \\ & + b_1^7 b_s \left\{ \sum_{i=0}^3 \sum_{j=0}^3 \left\langle S^{(2)}(\mathbf{x} + \mathbf{r}_i) \delta^{(2)}(\mathbf{x} + \mathbf{r}'_j + \mathbf{s}) \right. \right. \\ & \times \prod_{p=0, p \neq i}^3 \prod_{t=0, t \neq j}^3 \delta_{\text{lin.}}(\mathbf{x} + \mathbf{r}_p) \delta_{\text{lin.}}(\mathbf{x} + \mathbf{r}'_t + \mathbf{s}) \left. \right\rangle + \text{symm.} \Big\}. \quad (2.6) \end{aligned}$$

Above, we used the subscript 4,1L on the left-hand side to denote that we evaluate the 4PCF 1-loop covariance. This equation captures all possible permutations of the terms through the two summations and two products, ensuring that for each choice of  $i$ ,  $p \in \{0, 1, 2, 3\}$  must be distinct from  $i$ , and similarly, for each choice of  $j$ ,  $t \in \{0, 1, 2, 3\}$  must be distinct from  $j$ . In what follows, we display only the product over  $p$  and  $t$ , with the understanding that  $p \neq i$  and  $t \neq j$  are implicitly enforced. The first three terms are symmetric under the exchange of primed and unprimed vectors, whereas the last three terms are not. To restore the symmetry, an additional “+ symm.” has been included in the last three terms; we show an example of how to compute these terms below:

$$\begin{aligned}
& b_1^7 \frac{b_2}{2} \left\{ \sum_{i=0}^3 \sum_{j=0}^3 \left\langle \delta_{\text{lin.}}^2(\mathbf{x} + \mathbf{r}_i) \delta^{(2)}(\mathbf{x} + \mathbf{r}'_j + \mathbf{s}) \right. \right. \\
& \quad \times \prod_{p=0, p \neq i}^3 \prod_{t=0, t \neq j}^3 \delta_{\text{lin.}}(\mathbf{x} + \mathbf{r}_p) \delta_{\text{lin.}}(\mathbf{x} + \mathbf{r}'_t + \mathbf{s}) \left. \right\rangle + \text{symm.} \left. \right\} \\
& = b_1^7 \frac{b_2}{2} \left\{ \sum_{i=0}^3 \sum_{j=0}^3 \left\langle \delta_{\text{lin.}}^2(\mathbf{x} + \mathbf{r}_i) \delta^{(2)}(\mathbf{x} + \mathbf{r}'_j + \mathbf{s}) \right. \right. \\
& \quad \times \prod_{p=0, p \neq i}^3 \prod_{t=0, t \neq j}^3 \delta_{\text{lin.}}(\mathbf{x} + \mathbf{r}_p) \delta_{\text{lin.}}(\mathbf{x} + \mathbf{r}'_t + \mathbf{s}) \left. \right\rangle \\
& \quad + \sum_{i=0}^3 \sum_{j=0}^3 \left\langle \delta^{(2)}(\mathbf{x} + \mathbf{r}_i) \delta_{\text{lin.}}^2(\mathbf{x} + \mathbf{r}'_j + \mathbf{s}) \right. \\
& \quad \times \prod_{p=0, p \neq i}^3 \prod_{t=0, t \neq j}^3 \delta_{\text{lin.}}(\mathbf{x} + \mathbf{r}_p) \delta_{\text{lin.}}(\mathbf{x} + \mathbf{r}'_t + \mathbf{s}) \left. \right\rangle \left. \right\}. \tag{2.7}
\end{aligned}$$

We prove in Appendix A that the six terms in Eq. (2.6) may all be written in terms of a simple expression, using a generalization of the (Fourier space)  $F^{(2)}$  kernel that we develop there.

Using the result of Appendix A and rewriting the density contrast in terms of its inverse Fourier transform, the 1-loop covariance is:

$$\begin{aligned}
\text{Cov}_{4,1\text{L}}^{[2]}(\mathbf{R}, \mathbf{R}') & = \prod_{v=0}^3 \int_{\mathbf{s}} \int_{\mathbf{k}_v} \int_{\mathbf{k}'_v} \left[ e^{-i\mathbf{k}_v \cdot (\mathbf{x} + \mathbf{r}_v)} e^{-i\mathbf{k}'_v \cdot (\mathbf{x} + \mathbf{r}'_v + \mathbf{s})} \right] \\
& \quad \times \sum_{\mu, \beta} \sum_{i, j} \left\langle \tilde{\delta}_{\mu}^{(2)}(\mathbf{k}_i) \tilde{\delta}_{\beta}^{(2)}(\mathbf{k}'_j) \prod_{p, t} \tilde{\delta}_{\text{lin.}}(\mathbf{k}_p) \tilde{\delta}_{\text{lin.}}(\mathbf{k}'_t) \right\rangle, \tag{2.8}
\end{aligned}$$

where  $\mu$  and  $\beta$  run over  $\{0, 1, 2\}$  such that  $\{\tilde{\delta}_0^{(2)}, \tilde{\delta}_1^{(2)}, \tilde{\delta}_2^{(2)}\} = \{S^{(2)}, \tilde{\delta}^{(2)}, \tilde{\delta}_{\text{lin.}}^2\}$ , respectively. We have abbreviated the 3D integrals as:

$$\int_{\mathbf{s}} = \int \frac{d^3 \mathbf{s}}{V}, \quad \int_{\mathbf{k}} = \int \frac{d^3 \mathbf{k}}{(2\pi)^3} \quad \text{and} \quad \int_{\hat{\mathbf{k}}} = \int d\hat{\mathbf{k}}.$$

Expanding the second-order density of Eq. (2.8) using Eq. (A.6), we obtain:

$$\begin{aligned}
\text{Cov}_{4,1\text{L}}^{[2]}(\mathbf{R}, \mathbf{R}') &= \prod_{v=0}^3 \int_{\mathbf{s}} \int_{\mathbf{k}_v} \int_{\mathbf{k}'_v} \left[ e^{-i\mathbf{k}_v \cdot (\mathbf{x} + \mathbf{r}_v)} e^{-i\mathbf{k}'_v \cdot (\mathbf{x} + \mathbf{r}'_v + \mathbf{s})} \right] \\
&\times \sum_{\mu, \beta} \int d^3 \mathbf{q}_1 \int d^3 \mathbf{q}_2 \int d^3 \mathbf{q}'_1 \int d^3 \mathbf{q}'_2 W_{\mu}^{(2)}(\mathbf{q}_1, \mathbf{q}_2) \\
&\times W_{\beta}^{(2)}(\mathbf{q}'_1, \mathbf{q}'_2) \delta_{\text{D}}^{[3]}(\mathbf{k}_0 - \mathbf{q}_1 - \mathbf{q}_2) \delta_{\text{D}}^{[3]}(\mathbf{k}'_0 - \mathbf{q}'_1 - \mathbf{q}'_2) \\
&\times \left\langle \tilde{\delta}_{\text{lin.}}(\mathbf{q}_1) \tilde{\delta}_{\text{lin.}}(\mathbf{q}_2) \tilde{\delta}_{\text{lin.}}(\mathbf{q}'_1) \tilde{\delta}_{\text{lin.}}(\mathbf{q}'_2) \prod_{p,t=1}^3 \tilde{\delta}_{\text{lin.}}(\mathbf{k}_p) \tilde{\delta}_{\text{lin.}}(\mathbf{k}'_t) \right\rangle, \quad (2.9)
\end{aligned}$$

where the  $W^{(2)}$  kernel is defined in Eq. (A.7). The evaluation of the ensemble average of the density contrasts using Wick's theorem leads to five different possible configurations as shown in Figs. 1 and 4. Therefore, in the next section we develop the basic mathematical elements of the covariance.

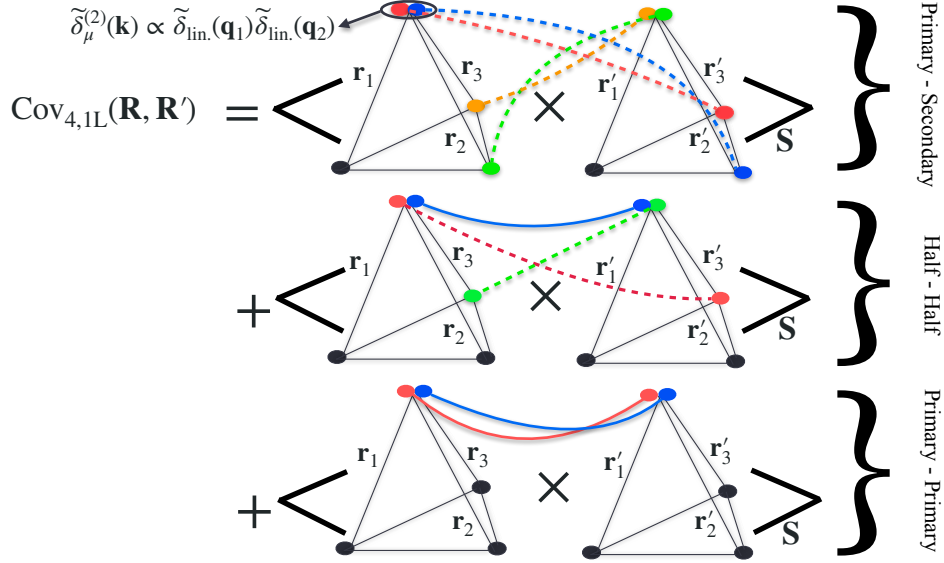


**Figure 1.** Illustration of the three different possible configurations of the fully-coupled covariance at 1-loop order. The three configurations at this order are: Primary-Secondary, Half-Half and Primary-Primary. The solid lines represent the contraction of two primary density contrasts via Wick's theorem; the dashed lines represent the contraction of a primary overdensity with a secondary one. We define the 'primary' points as those that contain the second-order densities and depict them in the above diagram with two colored dots. We define the 'secondary' points as those that contain the first-order densities and depict them with one black dot. The above diagram does not show Wick contractions between the leftover-secondary densities (black dots), but what results from them has been explicitly included and calculated in each of the sections below. The primary densities within each tetrahedron are  $\mathbf{q}_1, \mathbf{q}_2$  from left to right; likewise with the primed tetrahedron. In the main text, We introduce  $\mathbf{r}_0 = \mathbf{r}'_0 = 0$  to restore the symmetry between arguments of the calculations in §3.

Table of Coefficients		
Coefficient	Equation/Section	Definition
$C_{L_1, L_2, L_3}$	3.6	Coefficient of plane-wave expansion when projected onto the isotropic basis functions.
$\Upsilon_{L_1, L_2, L_3}$	3.7	Coefficient from the splitting of position-space-vector and wave-vector isotropic basis functions.
$c_{j,n}^{(\mu)}$	A.7	$W_{\delta_i}^{(2)}$ kernel coefficients.
$\mathcal{G}_{L_1, L_2, L_3}$	B.1	Coefficient from the integration of one 3-argument isotropic basis function.
$\hat{G}_{L_1, L_2, L_3}$	B.4	Coefficient from the integration of one 2-argument isotropic basis function times one spherical harmonic.
$\mathcal{H}_{L, L', L'', \ell}$	B.5	Coefficient from the integration of one 3-argument isotropic basis function times one spherical harmonic.
$\mathcal{J}_{L, L', L'', \ell, \ell''}$	B.6	Coefficient from the integration of one 3-argument isotropic basis function times two spherical harmonics.
$\overline{\mathcal{Q}}^{\Lambda, \Lambda_s, \Lambda'}$	§C	Coefficients from the evaluation of the $\hat{\mathbf{s}}$ integral for the five different configurations of the 1-loop covariance.
$\omega_{\ell, \ell'}$	D.7	Coefficient from the splitting of mixed-space 2-argument isotropic basis functions.

**Table 1.** Table with the coefficients relevant for the computation of the covariance. The first four coefficients have been taken from [13], although the fourth,  $c_{j,n}^{(\mu)}$  has been modified for the work in this paper.

### 3 Modeling the 1-Loop Covariance with Second-Order Densities

Before presenting the detailed derivations, we outline the structure of the second-order contributions to the 4PCF covariance. The full set of terms can be grouped into two categories: fully-connected and partially-connected configurations. In total, five distinct diagrammatic structures arise. Three of them belong to the fully-connected class, shown in Figure 1, while

the remaining two fall into the partially-connected class, illustrated in Figure 4.

The distinction between these categories is most easily seen in their diagrammatic representation. In the fully-connected case, Wick contractions link the two tetrahedra that define the covariance, ensuring that all density contrasts are connected across them. In contrast, in the partially-connected case, one loop is formed entirely within a single tetrahedron, leaving the connection between the two tetrahedra incomplete. We begin with the fully-connected configurations and then turn to the partially-connected ones.

### 3.1 Fully-Connected Terms

Within the class of fully-connected contributions, three distinct configurations arise, shown in Figure 1. We evaluate them in the order displayed: the primary–secondary, half–half, and primary–primary contractions. These labels indicate how the second-order (“primary”) density contrasts are paired with the linear (“secondary”) densities through Wick’s theorem. In the diagrams, solid colored lines represent Wick contractions between densities of the same type, while dotted lines denote contractions between a primary and a secondary field. Each configuration corresponds to a different way of distributing the second-order density insertions across the two tetrahedra, and together they exhaust all possible fully-connected structures. We begin with the primary-secondary configuration.

#### 3.1.1 Primary-Secondary Configuration

Using Wick’s theorem on Eq. (2.9) for the primary-secondary configuration shown in Fig. 1 results in:

$$\begin{aligned}
\text{Cov}_{4,1\text{L}}^{[2],\text{P-S}}(\mathbf{R}, \mathbf{R}') &= \prod_{v=0}^3 \int_{\mathbf{s}} \int_{\mathbf{k}_v} \int_{\mathbf{k}'_v} \left[ e^{-i\mathbf{k}_v \cdot (\mathbf{x} + \mathbf{r}_v)} e^{-i\mathbf{k}'_v \cdot (\mathbf{x} + \mathbf{r}'_v + \mathbf{s})} \right] \\
&\times \int d^3\mathbf{q}_1 \int d^3\mathbf{q}_2 \int d^3\mathbf{q}'_1 \int d^3\mathbf{q}'_2 W^{(2)}(\mathbf{q}_1, \mathbf{q}_2) \\
&\times W^{(2)}(\mathbf{q}'_1, \mathbf{q}'_2) \delta_{\text{D}}^{[3]}(\mathbf{k}_0 - \mathbf{q}_1 - \mathbf{q}_2) \delta_{\text{D}}^{[3]}(\mathbf{k}'_0 - \mathbf{q}'_1 - \mathbf{q}'_2) \\
&\times \left\langle \tilde{\delta}_{\text{lin.}}(\mathbf{q}_1) \tilde{\delta}_{\text{lin.}}(\mathbf{k}'_3) \right\rangle \left\langle \tilde{\delta}_{\text{lin.}}(\mathbf{q}_2) \tilde{\delta}_{\text{lin.}}(\mathbf{k}'_2) \right\rangle \left\langle \tilde{\delta}_{\text{lin.}}(\mathbf{q}'_1) \tilde{\delta}_{\text{lin.}}(\mathbf{k}_3) \right\rangle \\
&\times \left\langle \tilde{\delta}_{\text{lin.}}(\mathbf{q}'_2) \tilde{\delta}_{\text{lin.}}(\mathbf{k}_2) \right\rangle \left\langle \tilde{\delta}_{\text{lin.}}(\mathbf{k}_1) \tilde{\delta}_{\text{lin.}}(\mathbf{k}'_1) \right\rangle + 35 \text{ perms.}, \tag{3.1}
\end{aligned}$$

where 35 perms. indicates the other 35 combinations<sup>2</sup> from Wick’s theorem that we obtain for this primary-secondary structure. For brevity, we leave this out, but it is implicitly included into our calculations. Evaluating the ensemble averages as power spectra and performing the

---

<sup>2</sup>Finding the number of permutations is done in three steps. i) Choose one of the second-order densities in any of the two tetrahedra, then pair this second-order density with one of the linear densities from the other tetrahedron; one has 3 possibilities. ii) Repeat with the remaining second-order density; one has 2 possibilities. iii) Repeat with the opposite tetrahedron steps i) and ii); one has 6 possibilities. Total number of permutations =  $3 \times 2 \times 6 = 36$  perms.

integrals  $\mathbf{q}_s$  and  $\mathbf{q}'_s$  results in:

$$\begin{aligned} \text{Cov}_{4,1L}^{[2],\text{P-S}}(\mathbf{R}, \mathbf{R}') &= (2\pi)^{15} \prod_{v=0}^3 \int_{\mathbf{s}} \int_{\mathbf{k}_v} \int_{\mathbf{k}'_v} \left[ e^{-i\mathbf{k}_v \cdot (\mathbf{x} + \mathbf{r}_v)} e^{-i\mathbf{k}'_v \cdot (\mathbf{x} + \mathbf{r}'_v + \mathbf{s})} \right] \\ &\times \delta_D^{[3]}(\mathbf{k}_0 + \mathbf{k}'_2 + \mathbf{k}'_3) \delta_D^{[3]}(\mathbf{k}'_0 + \mathbf{k}_2 + \mathbf{k}_3) \delta_D^{[3]}(\mathbf{k}_1 + \mathbf{k}'_1) \\ &\times W^{(2)}(\mathbf{k}'_3, \mathbf{k}'_2) W^{(2)}(\mathbf{k}_3, \mathbf{k}_2) \\ &\times P_{\text{lin}}(k_2) P_{\text{lin}}(k_3) P_{\text{lin}}(k'_2) P_{\text{lin}}(k'_3) P_{\text{lin}}(k_1), \end{aligned} \quad (3.2)$$

where  $(2\pi)^{15}$  arises from expressing the five ensemble average product of Eq. (3.1) in terms of power spectra. By using the Dirac delta functions we obtain:

$$\begin{aligned} \text{Cov}_{4,1L}^{[2],\text{P-S}}(\mathbf{R}, \mathbf{R}') &= \int_{\mathbf{s}} \int_{\mathbf{k}_1} e^{-i\mathbf{k}_1 \cdot (\mathbf{r}_1 - \mathbf{s} - \mathbf{r}'_1)} P_{\text{lin}}(k_1) \\ &\times \int_{\mathbf{k}_3} e^{-i\mathbf{k}_3 \cdot (\mathbf{r}_3 - \mathbf{s} - \mathbf{r}'_0)} P_{\text{lin}}(k_3) \\ &\times \int_{\mathbf{k}'_3} e^{-i\mathbf{k}'_3 \cdot (\mathbf{r}'_3 + \mathbf{s} - \mathbf{r}_0)} P_{\text{lin}}(k'_3) \\ &\times \int_{\mathbf{k}_2} W^{(2)}(\mathbf{k}_2, \mathbf{k}_3) P_{\text{lin}}(k_2) e^{-i\mathbf{k}_2 \cdot (\mathbf{r}_2 - \mathbf{s} - \mathbf{r}'_0)} \\ &\times \int_{\mathbf{k}'_2} W^{(2)}(\mathbf{k}'_2, \mathbf{k}'_3) P_{\text{lin}}(k'_2) e^{-i\mathbf{k}'_2 \cdot (\mathbf{r}'_2 + \mathbf{s} - \mathbf{r}_0)}. \end{aligned} \quad (3.3)$$

To simplify the above result we will start by reducing the  $\mathbf{k}_2$  integral to have as low a dimension as possible :

$$I^{(2)}(\mathbf{r}_2, -\mathbf{s}, -\mathbf{r}'_0) \equiv \int_{\mathbf{k}_2} W^{(2)}(\mathbf{k}_2, \mathbf{k}_3) P(k_2) e^{-i\mathbf{k}_2 \cdot (\mathbf{r}_2 - \mathbf{s} - \mathbf{r}'_0)}. \quad (3.4)$$

We proceed by writing all the terms in the integrand in terms of the isotropic basis functions, which will allow us to separate the angular and radial parts; evaluating the rest of the  $\mathbf{k}$  and  $\mathbf{k}'$  integrals will follow the same procedure and their result is explicitly given in Eqs. (3.10)-(3.12). The second-order kernel  $W^{(2)}$  is already given in terms of the isotropic basis functions in Eq. (A.7).

In the same manner, the complex exponential can be expanded into this basis using the plane wave expansion [13]:

$$\begin{aligned} e^{-i\mathbf{k}_2 \cdot (\mathbf{r}_2 - \mathbf{s} - \mathbf{r}'_0)} &= (4\pi)^3 \sum_{L_2, L_{2s}, L'_{20}} C_{L_2, L_{2s}, L'_{20}} \Upsilon_{L_2, L_{2s}, L'_{20}} j_{L_2}(k_2 r_2) j_{L_{2s}}(k_2 s) \\ &\times j_{L'_{20}}(k_2 r'_0) \mathcal{P}_{L_2, L_{2s}, L'_{20}}(\widehat{\mathbf{k}}_2, \widehat{\mathbf{k}}_2, \widehat{\mathbf{k}}_2) \mathcal{P}_{L_2, L_{2s}, L'_{20}}(\widehat{\mathbf{r}}_2, -\widehat{\mathbf{s}}, -\widehat{\mathbf{r}}'_0). \end{aligned} \quad (3.5)$$

We define the PWE constants as:

$$C_{\ell'_1, \ell'_2, \ell'_3} \equiv i^{\ell'_1 + \ell'_2 + \ell'_3} \sqrt{(2\ell'_1 + 1)(2\ell'_2 + 1)(2\ell'_3 + 1)}, \quad (3.6)$$

and

$$\Upsilon_{L_1, L_2, L_3} = \frac{(-1)^{L_1 + L_2 + L_3}}{\sqrt{(2L_1 + 1)(2L_2 + 1)(2L_3 + 1)}}, \quad (3.7)$$

. Finally, with all of the terms in the isotropic basis, after evaluating the angular integrals we obtain:

$$I_{j,n}^{(2)}(\mathbf{r}_2, -\mathbf{s}, -\mathbf{r}'_0) = (4\pi)^2 \sum_{L_2, L_{2s}, L'_{20}} C_{L_2, L_{2s}, L'_{20}} \Upsilon_{L_2, L_{2s}, L'_{20}} \mathcal{H}_{L_2, L_{2s}, L'_{20}, j} \times g_{L_2, L_{2s}, L'_{20}}^{[n]}(r_2, s, r'_0) \mathcal{P}_{L_2, L_{2s}, L'_{20}}(\hat{\mathbf{r}}_2, -\hat{\mathbf{s}}, -\hat{\mathbf{r}}'_0), \quad (3.8)$$

where we have intentionally left out the  $j, n$  sums and factor of  $4\pi$  since they will also affect the result of the  $\mathbf{k}_3$  integral; to denote this, we have included the subscripts  $j, n$  on the left-hand side of the above equation. We reintroduce these sums in Eq. (3.14). The constant  $\mathcal{H}$  comes directly from evaluating the angular integral as shown in Eq. (B.5). The radial integral  $g$  is defined as:

$$g_{L, L', L''}^{[n]}(r, r', r'') \equiv \int \frac{dk}{2\pi^2} k^{n+2} j_L(kr) j_{L'}(kr') j_{L''}(kr'') P_{\text{lin}}(k). \quad (3.9)$$

Eq. (3.8) immediately allows us to evaluate the  $\mathbf{k}_3, \mathbf{k}'_2$  and  $\mathbf{k}'_3$  integrals as:

$$I_{j,n}^{(3)}(\mathbf{r}_3, -\mathbf{s}, -\mathbf{r}'_0) = (4\pi)^2 \sum_{L_3, L_{3s}, L'_{30}} C_{L_3, L_{3s}, L'_{30}} \Upsilon_{L_3, L_{3s}, L'_{30}} \mathcal{H}_{L_3, L_{3s}, L'_{30}, j} \times g_{L_3, L_{3s}, L'_{30}}^{[-n]}(r_3, s, r'_0) \mathcal{P}_{L_3, L_{3s}, L'_{30}}(\hat{\mathbf{r}}_3, -\hat{\mathbf{s}}, -\hat{\mathbf{r}}'_0), \quad (3.10)$$

$$I_{j',n'}^{(2')}(\mathbf{r}_0, -\mathbf{s}, -\mathbf{r}'_2) = (4\pi)^2 \sum_{L_{20}, L'_{2s}, L'_2} C_{L_{20}, L'_{2s}, L'_2} \Upsilon_{L_{20}, L'_{2s}, L'_2} \mathcal{H}_{L_{20}, L'_{2s}, L'_2, j'} \times g_{L_{20}, L'_{2s}, L'_2}^{[n']}(r_0, s, r'_2) \mathcal{P}_{L_{20}, L'_{2s}, L'_2}(\hat{\mathbf{r}}_0, -\hat{\mathbf{s}}, -\hat{\mathbf{r}}'_2), \quad (3.11)$$

$$I_{j',n'}^{(3')}(\mathbf{r}_0, -\mathbf{s}, -\mathbf{r}'_3) = (4\pi)^2 \sum_{L_0, L'_{3s}, L'_3} C_{L_0, L'_{3s}, L'_3} \Upsilon_{L_0, L'_{3s}, L'_3} \mathcal{H}_{L_0, L'_{3s}, L'_3, j'} \times g_{L_0, L'_{3s}, L'_3}^{[-n']} (r_0, s, r'_3) \mathcal{P}_{L_0, L'_{3s}, L'_3}(\hat{\mathbf{r}}_0, -\hat{\mathbf{s}}, -\hat{\mathbf{r}}'_3). \quad (3.12)$$

Next, we must evaluate the  $\mathbf{k}_1$  integral. To do so, we follow the same procedure as before but without the second-order kernel. This means that the evaluation of its angular integral will produce a modified Gaunt coefficient instead of an  $\mathcal{H}$  coefficient. We find:

$$I^{(1)}(\mathbf{r}_1, -\mathbf{r}'_1, -\mathbf{s}) = (4\pi)^2 \sum_{L_1, L_{1s}, L'_1} C_{L_1, L_{1s}, L'_1} \Upsilon_{L_1, L_{1s}, L'_1} \mathcal{G}_{L_1, L_{1s}, L'_1} \times g_{L_1, L_{1s}, L'_1}^{[0]}(r_1, s, r'_1) \mathcal{P}_{L_1, L_{1s}, L'_1}(\hat{\mathbf{r}}_1, -\hat{\mathbf{s}}, -\hat{\mathbf{r}}'_1), \quad (3.13)$$

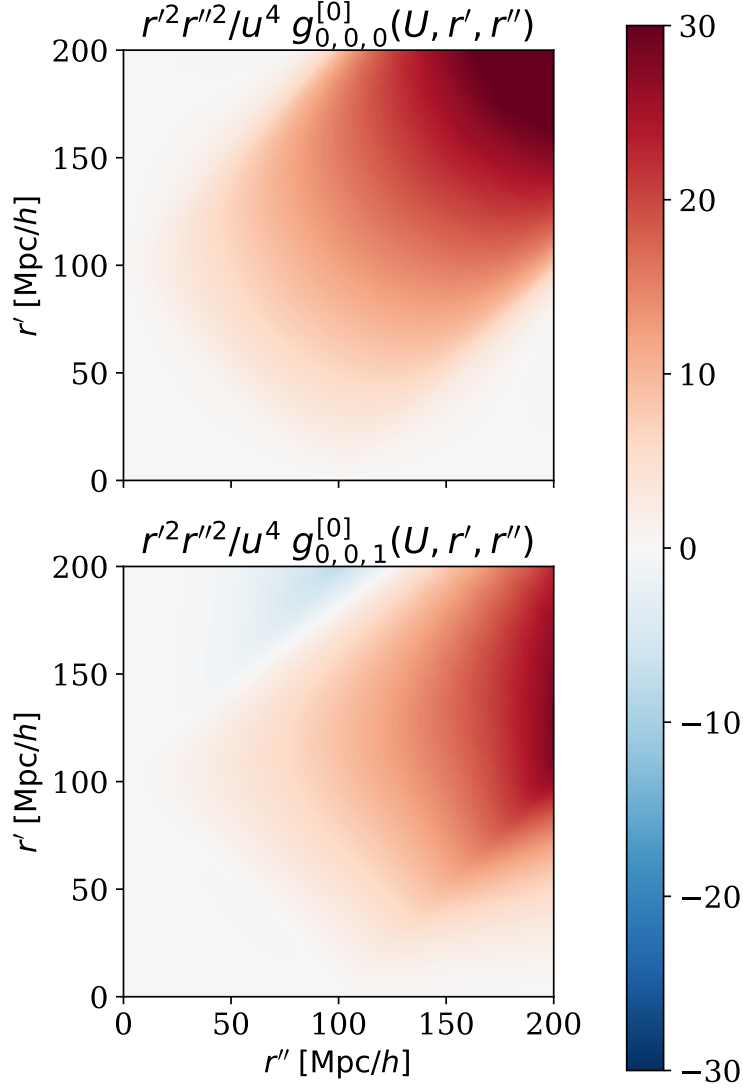


**Figure 2.** Here, we show Eq. (3.9) for fixed  $r' = U \equiv 100$  [Mpc/h],  $n' = 0$ ,  $\ell' = 0$ ,  $\ell = 0$  and  $L = \{0, 1\}$ . The plot has been taken from section 3 of [13]. The *upper panel* shows the integral for  $L = 0$ , while the *lower panel* shows the integral for  $L = 1$ . Since the 4PCF can be approximated as the square of the 2PCF on large scales,  $(\xi_0)^2(r) \sim (1/r^2)^2$ , we have weighted the integral by  $r^2 r_i^2 / u^4$ , with  $u \equiv 10$  [Mpc/h] to take out its fall-off. Both the *upper* and *lower* panel show the behavior of the integral creates a rectangular boundary. Analytical results with the power spectrum using a power law and explaining the rectangular boundaries ( $r' = r'' + U$ ,  $r' = -r'' + U$ , and  $r' = r'' - U$ ) have been obtained in [13]; further results are also evaluated in [5].

with  $\mathcal{G}$  defined in Eq. (B.1). Finally, after evaluating the  $\hat{\mathbf{s}}$  integral using Eq. (C.7), we

obtain:

$$\begin{aligned}
\text{Cov}_{4,1L}^{[2],\text{P-S}}(\mathbf{R}, \mathbf{R}') &= (2\pi)^{15} (4\pi)^{12} \sum_{\text{All}} \\
&\times c_{j,n}^{(\mu)} c_{j',n'}^{(\beta)} \overline{\mathcal{Q}}_{(\text{P-S})}^{\Lambda, \Lambda_s, \Lambda'} \\
&\times C_{L_1, L'_1, L_{1s}} \Upsilon_{L_1, L'_1, L_{1s}} \mathcal{G}_{L_1, L'_1, L_{1s}} \\
&\times C_{L_2, L_{2s}, L'_{20}} \Upsilon_{L_2, L_{2s}, L'_{20}} \mathcal{H}_{L_2, L_{2s}, L'_{20}, j} \\
&\times C_{L_3, L_{3s}, L'_{30}} \Upsilon_{L_3, L_{3s}, L'_{30}} \mathcal{H}_{L_3, L_{3s}, L'_{30}, j} \\
&\times C_{L'_2, L'_{2s}, L_{20}} \Upsilon_{L'_2, L'_{2s}, L_{20}} \mathcal{H}_{L'_2, L'_{2s}, L_{20}, j'} \\
&\times C_{L'_3, L'_{3s}, L_{30}} \Upsilon_{L'_3, L'_{3s}, L_{30}} \mathcal{H}_{L'_3, L'_{3s}, L_{30}, j'} \\
&\times S_{\{L\}, \text{P-S}}^{(\{L_{is}\})}(r_0, r'_0, r_1, r'_1, r_2, r'_2, r_3, r'_3) \\
&\times \mathcal{P}_\Lambda(\widehat{\mathbf{R}}) \mathcal{P}_{\Lambda'}(\widehat{\mathbf{R}}') + 35 \text{ perms.},
\end{aligned} \tag{3.14}$$

where the  $\Lambda$ ,  $\Lambda_s$  and  $\Lambda'$  momenta have been defined in §C.1. Table 1 provides the equations where each constant is defined. We have defined the radial integral  $S$  as:

$$\begin{aligned}
S_{\{L\}, \text{P-S}}^{(\{L_{is}\})}(r_0, r'_0, r_1, r'_1, r_2, r'_2, r_3, r'_3) \\
\equiv \int ds s^2 g_{L_1, L'_1, L_{1s}}^{[0]}(r_1, r'_1, s) g_{L_2, L_{2s}, L'_{20}}^{[n]}(r_2, s, r'_0) \\
\times g_{L_3, L_{3s}, L'_{30}}^{[-n]}(r_3, s, r'_0) g_{L'_2, L'_{2s}, L_{20}}^{[n']}(r'_2, s, r_0) g_{L'_3, L'_{3s}, L_{30}}^{[-n']}(r'_3, s, r_0).
\end{aligned} \tag{3.15}$$

The subscript  $\{L\}$  denotes the set of all angular momentum indices that affect one of the resulting variables (*i.e.*, the  $r_0, r'_0, \dots$  variables). The superscript  $(\{L_{is}\})$  denotes the set of all angular momentum indices that are coupled to  $s$  in the spherical Bessel functions.

### 3.1.2 Half-Half Configuration

Next, we analyze the half-half configuration. The name reflects the fact that its Wick contractions split evenly: one contraction joins two primary densities, while another pairs a primary with a secondary density. Using Wick's theorem on Eq. (2.9), which describes the half-half configuration shown in Fig. 1, we find:

$$\begin{aligned}
\text{Cov}_{4,1L}^{[2],\text{H-H}}(\mathbf{R}, \mathbf{R}') &= \prod_{v=0}^3 \int_{\mathbf{s}} \int_{\mathbf{k}_v} \int_{\mathbf{k}'_v} \left[ e^{-i\mathbf{k}_v \cdot (\mathbf{x} + \mathbf{r}_v)} e^{-i\mathbf{k}'_v \cdot (\mathbf{x} + \mathbf{r}'_v + \mathbf{s})} \right] \\
&\times \int d^3 \mathbf{q}_1 \int d^3 \mathbf{q}_2 \int d^3 \mathbf{q}'_1 \int d^3 \mathbf{q}'_2 W^{(2)}(\mathbf{q}_1, \mathbf{q}_2) \\
&\times W^{(2)}(\mathbf{q}'_1, \mathbf{q}'_2) \delta_D^{[3]}(\mathbf{k}_0 - \mathbf{q}_1 - \mathbf{q}_2) \delta_D^{[3]}(\mathbf{k}'_0 - \mathbf{q}'_1 - \mathbf{q}'_2) \\
&\times \langle \tilde{\delta}_{\text{lin.}}(\mathbf{q}_1) \tilde{\delta}_{\text{lin.}}(\mathbf{k}'_3) \rangle \langle \tilde{\delta}_{\text{lin.}}(\mathbf{q}_2) \tilde{\delta}_{\text{lin.}}(\mathbf{q}'_1) \rangle \langle \tilde{\delta}_{\text{lin.}}(\mathbf{q}'_2) \tilde{\delta}_{\text{lin.}}(\mathbf{k}_3) \rangle \\
&\times \langle \tilde{\delta}_{\text{lin.}}(\mathbf{k}_1) \tilde{\delta}_{\text{lin.}}(\mathbf{k}'_1) \rangle \langle \tilde{\delta}_{\text{lin.}}(\mathbf{k}_2) \tilde{\delta}_{\text{lin.}}(\mathbf{k}'_2) \rangle + 89 \text{ perms.},
\end{aligned} \tag{3.16}$$

where 89 perms. indicates the other 35 combinations<sup>3</sup> due to Wick's theorem that we can obtain for this primary-secondary structure. For brevity, we leave this out, but it is implicitly

<sup>3</sup>Finding the number of permutations is done in four steps. i) Choose one of the second-order densities in either of the two tetrahedra, then pair this second-order density with any densities from the other tetrahedron;

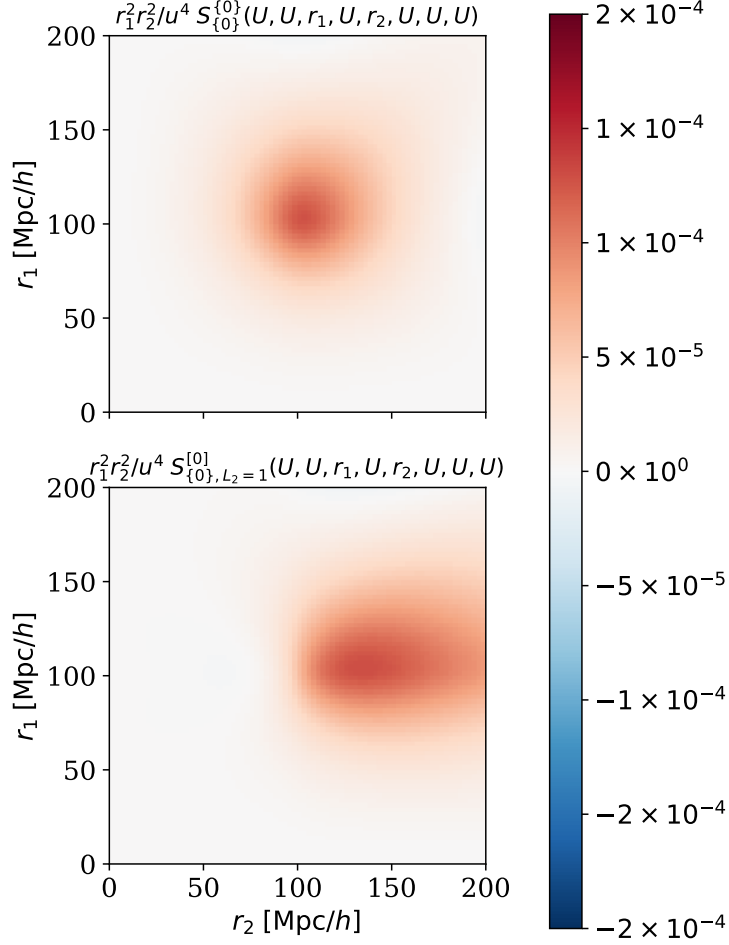


**Figure 3.** Here, we show Eqs. (3.15), (3.22) and (3.28) with fixed variables at  $U \equiv 100$  [Mpc/h], except for  $r_1$  and  $r_2$ . We also chose to evaluate  $n' = n = 0$  and all angular momentum  $\{L\} = 0$ , except for  $L_2 = \{0, 1\}$ . The *upper panel* shows the integral for  $L_2 = 0$ , while the *lower panel* shows the integral for  $L_2 = 1$ . Since the 4PCF can be approximated as the square of the 2PCF on large scales,  $(\xi_0)^2(r) \sim (1/r^2)^2$ , we have weighted the integral by  $r^2 r_i^2 / u^4$ , with  $u \equiv 10$  [Mpc/h], to take out its fall-off. The  $S$  integral is composed of the intermediate radial integrals,  $g$ , which reveals a rectangular boundary as shown in Fig. 2. The integration of the different rectangular boundaries creates the oval-shaped regions shown in both panels. Analytical results for similar radial integral with the power spectrum using a power law have been obtained in [13].

included into our calculations. Since the  $\mathbf{k}_1$ ,  $\mathbf{k}_2$ ,  $\mathbf{k}'_1$ , and  $\mathbf{k}'_2$  integrals do not depend on any second-order kernel, evaluating them will give the same result as in Eq. (3.13).

---

one has 5 possibilities. ii) Pair the remaining second-order density with any of the linear densities in the other tetrahedron; one has 3 possibilities. iii) In the other tetrahedron, pair the remaining second-order density with any of the linear densities in the first tetrahedron; one has 3 possibilities. iv) Choose one of the linear densities in any of the two tetrahedra, then pair this density with a linear density in the other tetrahedron; one has 2 possibilities. Total number of permutations =  $5 \times 3 \times 3 \times 2 = 90$  perms.

Then, performing the  $\mathbf{q}_1$ ,  $\mathbf{q}_2$ ,  $\mathbf{q}'_2$ ,  $\mathbf{k}_0$  and  $\mathbf{k}'_0$  integrals results in:

$$\begin{aligned} \text{Cov}_{4,1\text{L}}^{[2],\text{H-H}}(\mathbf{R}, \mathbf{R}') &= (2\pi)^{15} \int_{\mathbf{s}} I^{(1)}(\mathbf{r}_1, -\mathbf{s}, -\mathbf{r}'_1) I^{(2)}(\mathbf{r}_2, -\mathbf{s}, -\mathbf{r}'_2) \\ &\quad \times \int_{\mathbf{k}_3} \int_{\mathbf{k}'_3} \int_{\mathbf{q}'_1} \left[ e^{-i\mathbf{k}_3 \cdot (\mathbf{r}_3 - \mathbf{s} - \mathbf{r}'_0)} e^{-i\mathbf{k}'_3 \cdot (\mathbf{r}'_3 + \mathbf{s} - \mathbf{r}_0)} e^{-i\mathbf{q}'_1 \cdot (\mathbf{r}'_0 - \mathbf{r}_0 + \mathbf{s})} \right] \\ &\quad \times W^{(2)}(\mathbf{q}'_1, -\mathbf{k}_3) W^{(2)}(\mathbf{q}'_1, \mathbf{k}'_3) P_{\text{lin}}(q'_1) P_{\text{lin}}(k'_3) P_{\text{lin}}(k_3). \end{aligned} \quad (3.17)$$

Expressing the second-order kernels in the isotropic basis as in Eq.(A.7), and performing the same analysis as in Eqs. (3.4)-(3.8) for the  $\mathbf{k}_3$ ,  $\mathbf{k}'_3$  and  $\mathbf{q}'_1$  integrals, we obtain:

$$\begin{aligned} I_{j,n}^{(3)}(\mathbf{r}_3, -\mathbf{s}, -\mathbf{r}'_0) &= (4\pi)^2 \sum_{L_3, L_{3s}, L'_{30}} C_{L_3, L_{3s}, L'_{30}} \Upsilon_{L_3, L_{3s}, L'_{30}} \mathcal{H}_{L_3, L_{3s}, L'_{30}, j} \\ &\quad \times g_{L_3, L_{3s}, L'_{30}}^{[-n]}(r_3, s, r'_0) \mathcal{P}_{L_3, L_{3s}, L'_{30}}(\hat{\mathbf{r}}_3, -\hat{\mathbf{s}}, -\hat{\mathbf{r}}'_0), \end{aligned} \quad (3.18)$$

$$\begin{aligned} I_{j',n'}^{(3')}(\mathbf{r}'_3, \mathbf{s}, -\mathbf{r}_0) &= (4\pi)^2 \sum_{L'_3, L'_{3s}, L_{30}} C_{L'_3, L'_{3s}, L_{30}} \Upsilon_{L'_3, L'_{3s}, L_{30}} \mathcal{H}_{L'_3, L'_{3s}, L_{30}, j'} \\ &\quad \times g_{L'_3, L'_{3s}, L_{30}}^{[-n']}(\mathbf{r}'_3, \mathbf{s}, r_0) \mathcal{P}_{L'_3, L'_{3s}, L_{30}}(\hat{\mathbf{r}}'_3, \hat{\mathbf{s}}, -\hat{\mathbf{r}}_0), \end{aligned} \quad (3.19)$$

$$\begin{aligned} I_{j',n'}^{(q'_1)}(\mathbf{r}'_0, \mathbf{s}, -\mathbf{r}_0) &= (4\pi)^2 \sum_{L'_{q'_0}, L'_{qs}, L_{q0}} C_{L'_{q'_0}, L'_{qs}, L_{q0}} \Upsilon_{L'_{q'_0}, L'_{qs}, L_{q0}} \mathcal{J}_{L'_{q'_0}, L'_{qs}, L_{q0}, j, j'} \\ &\quad \times g_{L'_{q'_0}, L'_{qs}, L_{q0}}^{[n+n']}(\mathbf{r}'_0, \mathbf{s}, r_0) \mathcal{P}_{L'_{q'_0}, L'_{qs}, L_{q0}}(\hat{\mathbf{r}}'_0, \hat{\mathbf{s}}, -\hat{\mathbf{r}}_0), \end{aligned} \quad (3.20)$$

where evaluating the angular integral for  $\mathbf{q}'_1$  resulted in the constant  $\mathcal{J}$ . This integral involved the evaluation of one 3-argument isotropic basis function and two spherical harmonics, as shown in Eq. (B.6). Therefore, the half-half configuration results in:

$$\begin{aligned} \text{Cov}_{4,1\text{L}}^{[2],\text{H-H}}(\mathbf{R}, \mathbf{R}') &= (2\pi)^{15} (4\pi)^{12} \sum_{\text{All}} \\ &\quad \times c_{j,n}^{(\mu)} c_{j',n'}^{(\beta)} \overline{\mathcal{Q}}_{(\text{H-H})}^{\Lambda, \Lambda_s, \Lambda'} \\ &\quad \times C_{L_1, L'_1, L_{1s}} \Upsilon_{L_1, L'_1, L_{1s}} \mathcal{G}_{L_1, L'_1, L_{1s}} \\ &\quad \times C_{L_2, L'_2, L_{2s}} \Upsilon_{L_2, L'_2, L_{2s}} \mathcal{G}_{L_2, L'_2, L_{2s}} \\ &\quad \times C_{L_3, L_{3s}, L'_{30}} \Upsilon_{L_3, L_{3s}, L'_{30}} \mathcal{H}_{L_3, L_{3s}, L'_{30}, j} \\ &\quad \times C_{L'_3, L'_{3s}, L_{30}} \Upsilon_{L'_3, L'_{3s}, L_{30}} \mathcal{H}_{L'_3, L'_{3s}, L_{30}, j'} \\ &\quad \times C_{L'_{q'_0}, L'_{qs}, L_{q0}} \Upsilon_{L'_{q'_0}, L'_{qs}, L_{q0}} \mathcal{J}_{L'_{q'_0}, L'_{qs}, L_{q0}, j, j'} \\ &\quad \times S_{\{L\}, \text{H-H}}^{\{L_{is}\}}(r_0, r'_0, r_1, r'_1, r_2, r'_2, r_3, r'_3) \\ &\quad \times \mathcal{P}_{\Lambda}(\hat{\mathbf{R}}) \mathcal{P}_{\Lambda'}(\hat{\mathbf{R}}') + 89 \text{ perms.}, \end{aligned} \quad (3.21)$$

where the  $\Lambda$ ,  $\Lambda_s$  and  $\Lambda'$  momenta have been defined in §C.2. Table 1 provides the equation where all the constants have been defined. We have defined the radial integral  $S$  as:

$$\begin{aligned} S_{\{L\}, \text{H-H}}^{(\{L_{is}\})}(r_0, r'_0, r_1, r'_1, r_2, r'_2, r_3, r'_3) \\ \equiv \int ds s^2 g_{L_1, L'_1, L_1 s}^{[0]}(r_1, r'_1, s) g_{L_2, L'_2, L_2 s}^{[0]}(r_2, r'_2, s) \\ \times g_{L_3, L_{3s}, L'_{30}}^{[-n]}(r_3, s, r'_0) g_{L'_3, L'_{3s}, L_{30}}^{[-n']}(r'_3, s, r_0) g_{L'_{q_0}, L'_{qs}, L_{q_0}}^{[n+n']}(r'_2, s, r_0). \end{aligned} \quad (3.22)$$

The subscript  $\{L\}$  denotes the set of all angular momentum indices that affect one of the resulting variables (*i.e.*, the  $r_0, r'_0, \dots$  variables). The superscript  $(\{L_{is}\})$  denotes the set of all angular momentum indices that are coupled to  $s$  in the spherical Bessel functions.

### 3.1.3 Primary-Primary Configuration

Using Wick's theorem on Eq. (2.9), which describes the Primary-Primary configuration shown in Fig. 1, we find:

$$\begin{aligned} \text{Cov}_{4, \text{1L}}^{[2], \text{P-P}}(\mathbf{R}, \mathbf{R}') &= \prod_{v=0}^3 \int_{\mathbf{s}} \int_{\mathbf{k}_v} \int_{\mathbf{k}'_v} \left[ e^{-i\mathbf{k}_v \cdot (\mathbf{x} + \mathbf{r}_v)} e^{-i\mathbf{k}'_v \cdot (\mathbf{x} + \mathbf{r}'_v + \mathbf{s})} \right] \\ &\times \int d^3 \mathbf{q}_1 \int d^3 \mathbf{q}_2 \int d^3 \mathbf{q}'_1 \int d^3 \mathbf{q}'_2 W^{(2)}(\mathbf{q}_1, \mathbf{q}_2) \\ &\times W^{(2)}(\mathbf{q}'_1, \mathbf{q}'_2) \delta_{\text{D}}^{[3]}(\mathbf{k}_0 - \mathbf{q}_1 - \mathbf{q}_2) \delta_{\text{D}}^{[3]}(\mathbf{k}'_0 - \mathbf{q}'_1 - \mathbf{q}'_2) \\ &\times \langle \tilde{\delta}_{\text{lin.}}(\mathbf{q}_1) \tilde{\delta}_{\text{lin.}}(\mathbf{q}'_1) \rangle \langle \tilde{\delta}_{\text{lin.}}(\mathbf{q}_2) \tilde{\delta}_{\text{lin.}}(\mathbf{q}'_2) \rangle \langle \tilde{\delta}_{\text{lin.}}(\mathbf{k}_1) \tilde{\delta}_{\text{lin.}}(\mathbf{k}'_1) \rangle \\ &\times \langle \tilde{\delta}_{\text{lin.}}(\mathbf{k}_2) \tilde{\delta}_{\text{lin.}}(\mathbf{k}'_2) \rangle \langle \tilde{\delta}_{\text{lin.}}(\mathbf{k}_3) \tilde{\delta}_{\text{lin.}}(\mathbf{k}'_3) \rangle + 11 \text{ perms.}, \end{aligned} \quad (3.23)$$

where 11 perms. indicates the other 11 combinations<sup>4</sup> of Wick's theorem that we can obtain for this primary-primary structure. For brevity, we leave this out, but it is implicitly included into our calculations. Since the  $\mathbf{k}_1, \mathbf{k}_2, \mathbf{k}_3, \mathbf{k}'_1, \mathbf{k}'_2$ , and  $\mathbf{k}'_3$  integrals do not contain any second-order kernel, evaluating them will give the same result as in Eq. (3.13).

Then, performing the  $\mathbf{q}'_1, \mathbf{q}'_2, \mathbf{k}'_0$ , and  $\mathbf{k}_0$  integrals yields:

$$\begin{aligned} \text{Cov}_{4, \text{1L}}^{[2], \text{P-P}}(\mathbf{R}, \mathbf{R}') &= (2\pi)^{15} \int_{\mathbf{s}} I^{(1)}(\mathbf{r}_1, -\mathbf{r}'_1, -\mathbf{s}) I^{(2)}(\mathbf{r}_2, -\mathbf{r}'_2, -\mathbf{s}) \\ &\times I^{(3)}(\mathbf{r}_3, -\mathbf{r}'_3, -\mathbf{s}) \int_{\mathbf{q}_1} \int_{\mathbf{q}_2} \left[ e^{-i\mathbf{q}_1 \cdot (\mathbf{r}_0 - \mathbf{r}'_0 - \mathbf{s})} e^{-i\mathbf{q}_2 \cdot (\mathbf{r}_0 - \mathbf{r}'_0 - \mathbf{s})} \right] \\ &\times W^{(2)}(\mathbf{q}_1, \mathbf{q}_2) W^{(2)}(\mathbf{q}_1, \mathbf{q}_2) P_{\text{lin}}(q_1) P_{\text{lin}}(q_2). \end{aligned} \quad (3.24)$$

Expressing the two second-order kernels in terms of the isotropic basis function as in Eq. (A.7), and performing the same analysis as in Eqs. (3.4)-(3.8) for the  $\mathbf{q}_1$ , and  $\mathbf{q}_2$  integrals,

---

<sup>4</sup>Finding the number of permutations is done in three steps. i) Choose one of the second-order densities in either of the two tetrahedra, then pair this second-order density with another second-order density from the other tetrahedron; one has 2 possibilities. ii) Pair the remaining second-order density with the other second-order density in the other tetrahedron; one has 1 possibilities. iii) Pair the remaining linear densities with a linear density in the other tetrahedron; one has 6 possibilities. Total number of permutations =  $2 \times 1 \times 6 = 12$  perms.

we obtain:

$$I_{j,j',n,n'}^{(q_1)}(\mathbf{r}_0, -\mathbf{r}'_0, -\mathbf{s}) = (4\pi)^2 \sum_{L_{01}, L'_{01}, L'_{1qs}} C_{L_{01}, L'_{01}, L'_{1qs}} \Upsilon_{L_{01}, L'_{01}, L'_{1qs}} \mathcal{J}_{L_{01}, L'_{01}, L'_{1qs}, j, j'} \times g_{L_{01}, L'_{01}, L'_{1qs}}^{[n+n']} (r_0, r'_0, s) \mathcal{P}_{L_{01}, L'_{01}, L'_{1qs}}(\hat{\mathbf{r}}_0, -\hat{\mathbf{r}}'_0, -\hat{\mathbf{s}}), \quad (3.25)$$

and

$$I_{j,j',n,n'}^{(q_2)}(\mathbf{r}_0, -\mathbf{r}'_0, -\mathbf{s}) = (4\pi)^2 \sum_{L_{02}, L'_{02}, L'_{2qs}} C_{L_{02}, L'_{02}, L'_{2qs}} \Upsilon_{L_{02}, L'_{02}, L'_{2qs}} \mathcal{J}_{L_{02}, L'_{02}, L'_{2qs}, j, j'} \times g_{L_{01}, L'_{01}, L'_{2qs}}^{[-n-n']} (r_0, r'_0, s) \mathcal{P}_{L_{02}, L'_{02}, L'_{2qs}}(\hat{\mathbf{r}}_0, -\hat{\mathbf{r}}'_0, -\hat{\mathbf{s}}), \quad (3.26)$$

where the evaluation of the angular integrals  $\mathbf{q}'_1$  and  $\mathbf{q}'_2$  resulted in the constant  $\mathcal{J}$ . This integral involved the evaluation of one 3-argument isotropic basis function and two spherical harmonics, as shown in Eq. (B.6). Therefore, the primary-primary configuration, results in:

$$\begin{aligned} \text{Cov}_{4,1\text{L}}^{[2], \text{P-P}}(\mathbf{R}, \mathbf{R}') &= (2\pi)^{15} (4\pi)^{12} \sum_{\text{All}} \\ &\times c_{j,n}^{(\mu)} c_{j',n'}^{(\beta)} \overline{\mathcal{Q}}_{(\text{P-P})}^{\Lambda, \Lambda_s, \Lambda'} \\ &\times C_{L_1, L'_1, L_{1s}} \Upsilon_{L_1, L'_1, L_{1s}} \mathcal{G}_{L_1, L'_1, L_{1s}} \\ &\times C_{L_2, L'_2, L_{2s}} \Upsilon_{L_2, L'_2, L_{2s}} \mathcal{G}_{L_2, L'_2, L_{2s}} \\ &\times C_{L_3, L_{3s}, L'_{30}} \Upsilon_{L_3, L_{3s}, L'_{30}} \mathcal{G}_{L_3, L_{3s}, L'_{30}, j} \\ &\times C_{L_{01}, L'_{01}, L'_{1qs}} \Upsilon_{L_{01}, L'_{01}, L'_{1qs}} \mathcal{J}_{L_{01}, L'_{01}, L'_{1qs}, j, j'} \\ &\times C_{L_{02}, L'_{02}, L'_{2qs}} \Upsilon_{L_{02}, L'_{02}, L'_{2qs}} \mathcal{J}_{L_{02}, L'_{02}, L'_{2qs}, j, j'} \\ &\times S_{\{L\}, \text{P-P}}^(\{L_{is}\}) (r_0, r'_0, r_1, r'_1, r_2, r'_2, r_3, r'_3) \\ &\times \mathcal{P}_\Lambda(\hat{\mathbf{R}}) \mathcal{P}_{\Lambda'}(\hat{\mathbf{R}}') + 11 \text{ perms.}, \end{aligned} \quad (3.27)$$

where the  $\Lambda$ ,  $\Lambda_s$  and  $\Lambda'$  momenta have been defined in §C.3. Table 1 provides the equation where all the constants have been defined. We have defined the radial integral  $S$  as:

$$\begin{aligned} S_{\{L\}, \text{P-P}}^(\{L_{is}\}) (r_0, r'_0, r_1, r'_1, r_2, r'_2, r_3, r'_3) \\ \equiv \int ds s^2 g_{L_1, L'_1, L_{1s}}^{[0]}(r_1, r'_1, s) g_{L_2, L'_2, L_{2s}}^{[0]}(r_2, r'_2, s) \\ \times g_{L_3, L'_3, L_{3s}}^{[-n]}(r_3, r'_3, s) g_{L_{01}, L'_{01}, L_{1qs}}^{[n+n']} (r_0, r'_0, s) g_{L_{02}, L'_{02}, L_{2qs}}^{[-n-n']} (r_2, r'_2, s). \end{aligned} \quad (3.28)$$

The subscript  $\{L\}$  denotes the set of all angular momentum indices that affect one of the resulting variables (*i.e.*, the  $r_0, r'_0, \dots$  variables). The superscript  $(\{L_{is}\})$  denotes the set of all angular momentum indices that are coupled to  $s$  in the spherical Bessel functions.

### 3.2 Partially-Connected Terms

As demonstrated in Appendix E, the 1-loop covariance introduces partially-connected (PC) terms. There are two possible partially-connected configurations as shown in Figure 4. These

arise when one of the second-order (primary) densities is Wick-contracted with a linear (secondary) density inside the same tetrahedron, forming an internal loop. As a result, the connection between the two tetrahedra is incomplete, in contrast to the fully-connected case. The two possible structures are labeled PC-Primary-Secondary and PC-Half-Half, and we evaluate them in this order. In the diagrams, solid lines again denote contractions between densities of the same order, while dotted lines indicate contractions between primary and secondary fields. Together, these two cases exhaust all possible partially-connected structures at tenth order in the linear density field.

$$\begin{aligned}
\widetilde{\delta}_\mu^{(2)}(\mathbf{k}) \propto \widetilde{\delta}_{\text{lin.}}(\mathbf{q}_1) \widetilde{\delta}_{\text{lin.}}(\mathbf{q}_2) & \leftarrow \text{Diagram 1} \\
\text{Cov}_{4,1\text{L}}(\mathbf{R}, \mathbf{R}') = & \left\langle \text{Diagram 1} \right\rangle \times \left\langle \text{Diagram 2} \right\rangle \left. \vphantom{\left\langle \text{Diagram 1} \right\rangle} \right\} \text{PC - Primary - Secondary} \\
& + \left\langle \text{Diagram 3} \right\rangle \times \left\langle \text{Diagram 4} \right\rangle \left. \vphantom{\left\langle \text{Diagram 1} \right\rangle} \right\} \text{PC - Half - Half}
\end{aligned}$$

**Figure 4.** Illustration of the two different possible configurations of the partially-connected covariance at 1-loop order. They are: PC-Primary-Secondary and PC-Half-Half. The solid lines represent the contraction of two primary density contrasts via Wick’s theorem; the dashed lines represent the contraction of a primary overdensity with a secondary one. We define the ‘primary’ points with those that contain the second-order densities and depict them in the above diagram with two colored dots. We define the ‘secondary’ points with those that contain the first-order densities and depict them with one black dot. The above diagram does not show Wick contractions between the leftover-secondary densities (black dots), but what results from them has been explicitly included and calculated in each of the sections below. This figure visually illustrates that the partially-connected terms lack Wick contractions between all densities of the two tetrahedrons.

### 3.2.1 PC-Primary-Secondary Configuration

We begin the analysis of the PC-primary-secondary configuration as shown in Fig. 4. Using Wick's theorem for the PC-primary-secondary configuration on Eq. (2.9) results in:

$$\begin{aligned}
\text{Cov}_{4,1L}^{[2],\text{PC-P-S}}(\mathbf{R}, \mathbf{R}') &= \prod_{v=0}^3 \int_{\mathbf{s}} \int_{\mathbf{k}_v} \int_{\mathbf{k}'_v} \left[ e^{-i\mathbf{k}_v \cdot (\mathbf{x} + \mathbf{r}_v)} e^{-i\mathbf{k}'_v \cdot (\mathbf{x} + \mathbf{r}'_v + \mathbf{s})} \right] \\
&\times \int d^3 \mathbf{q}_1 \int d^3 \mathbf{q}_2 \int d^3 \mathbf{q}'_1 \int d^3 \mathbf{q}'_2 W^{(2)}(\mathbf{q}_1, \mathbf{q}_2) \\
&\times W^{(2)}(\mathbf{q}'_1, \mathbf{q}'_2) \delta_D^{[3]}(\mathbf{k}_0 - \mathbf{q}_1 - \mathbf{q}_2) \delta_D^{[3]}(\mathbf{k}'_0 - \mathbf{q}'_1 - \mathbf{q}'_2) \\
&\times \langle \tilde{\delta}_{\text{lin.}}(\mathbf{q}_1) \tilde{\delta}_{\text{lin.}}(\mathbf{k}_1) \rangle \langle \tilde{\delta}_{\text{lin.}}(\mathbf{q}_2) \tilde{\delta}_{\text{lin.}}(\mathbf{k}_2) \rangle \langle \tilde{\delta}_{\text{lin.}}(\mathbf{q}'_1) \tilde{\delta}_{\text{lin.}}(\mathbf{k}'_1) \rangle \\
&\times \langle \tilde{\delta}_{\text{lin.}}(\mathbf{q}'_2) \tilde{\delta}_{\text{lin.}}(\mathbf{k}'_2) \rangle \langle \tilde{\delta}_{\text{lin.}}(\mathbf{k}_3) \tilde{\delta}_{\text{lin.}}(\mathbf{k}'_3) \rangle + 35 \text{ perm.}, \tag{3.29}
\end{aligned}$$

where 35 perm. indicates the other 35 combinations<sup>5</sup> of Wick's theorem that we can obtain for this structure. For brevity, we leave this out, but it is implicitly included into our calculations. Evaluating the ensemble average as power spectra and performing the integrals  $\mathbf{q}_s$ ,  $\mathbf{q}'_s$ ,  $\mathbf{k}_0$ ,  $\mathbf{k}'_0$  and  $\mathbf{k}_3$  by taking advantage of the Dirac delta functions, we obtain:

$$\begin{aligned}
\text{Cov}_{4,1L}^{[2],\text{PC-P-S}}(\mathbf{R}, \mathbf{R}') &= \int_{\mathbf{s}} I^{(3)}(\mathbf{r}_3, -\mathbf{s}, -\mathbf{r}'_3) \\
&\times \int_{\mathbf{k}_1} e^{-i\mathbf{k}_1 \cdot (\mathbf{r}_1 - \mathbf{r}_0)} P_{\text{lin}}(k_1) \\
&\times \int_{\mathbf{k}'_1} e^{-i\mathbf{k}'_1 \cdot (\mathbf{r}'_1 - \mathbf{r}'_0)} P_{\text{lin}}(k'_1) \\
&\times \int_{\mathbf{k}_2} W^{(2)}(\mathbf{k}_1, \mathbf{k}_2) P_{\text{lin}}(k_2) e^{-i\mathbf{k}_2 \cdot (\mathbf{r}_2 - \mathbf{r}_0)} \\
&\times \int_{\mathbf{k}'_2} W^{(2)}(\mathbf{k}'_1, \mathbf{k}'_2) P_{\text{lin}}(k'_2) e^{-i\mathbf{k}'_2 \cdot (\mathbf{r}'_2 - \mathbf{r}'_0)}, \tag{3.30}
\end{aligned}$$

where we have used the same definition of Eq. (3.13) on  $I^{(3)}$ ; we changed the number in parentheses from 1  $\rightarrow$  3 to represent the result from the integral of  $\mathbf{k}_3$ .

We obtain the results for the remaining four integrals by expanding the exponential using Eq. (D.6), and the second-order kernel with Eq. (A.7):

$$I_{j,n}^{(2)}(\mathbf{r}_0, \mathbf{r}_2) = (4\pi) \sum_{L_{k_2}, L_{20}} w_{L_{k_2}, L_{20}} \hat{G}_{L_{20}, L_{20}, j} f_{L_{20}, L_{20}}^{[n]}(r_0, r_2) \mathcal{P}_{L_{20}}(\hat{\mathbf{r}}_0, \hat{\mathbf{r}}_2), \tag{3.31}$$

$$I_{j',n'}^{(2p)}(\mathbf{r}'_0, \mathbf{r}'_2) = (4\pi) \sum_{L'_{k'_2}, L'_{20}} w_{L'_{k'_2}, L'_{20}} \hat{G}_{L'_{20}, L'_{20}, j'} f_{L'_{20}, L'_{20}}^{[n']} (r_0, r_2) \mathcal{P}_{L'_{20}}(\hat{\mathbf{r}}'_0, \hat{\mathbf{r}}'_2), \tag{3.32}$$

---

<sup>5</sup>Finding the number of permutations is done in four steps. i) Choose one of the second-order densities in either of the two tetrahedra, then pair this second-order density with any linear density from the same tetrahedron; one has 3 possibilities. ii) Pair the remaining second-order density with any of the linear densities in the same tetrahedron; one has 2 possibilities. iii) Repeat i) and ii) in the other tetrahedron; one has 6 possibilities. Total number of permutations =  $3 \times 2 \times 6 = 36$  perms.

$$I_{j,n}^{(1)}(\mathbf{r}_0, \mathbf{r}_1) = (4\pi) \sum_{L_{k_1}, L_{10}} w_{L_{k_1}, L_{10}} \widehat{G}_{L_{10}, L_{10}, j} f_{L_{10}, L_{10}}^{[-n]}(r_0, r_1) \mathcal{P}_{L_{10}}(\widehat{\mathbf{r}}_0, \widehat{\mathbf{r}}_1), \quad (3.33)$$

$$I_{j',n'}^{(1p)}(\mathbf{r}'_0, \mathbf{r}'_1) = (4\pi) \sum_{L'_{k_1}, L'_{10}} w_{L'_{k_1}, L'_{10}} \widehat{G}_{L'_{10}, L'_{10}, j'} f_{L'_{10}, L'_{10}}^{[-n']}(\mathbf{r}'_0, \mathbf{r}'_1) \mathcal{P}_{L'_{10}}(\widehat{\mathbf{r}}'_0, \widehat{\mathbf{r}}'_1), \quad (3.34)$$

where we have defined  $\widehat{G}$  in Eq. (B.4),  $w$  in Eq. (D.6), and the radial integral as:

$$f_{\ell,\ell'}^{[n]}(r, r') \equiv \int \frac{dk}{2\pi^2} k^{n+2} j_\ell(kr) j_{\ell'}(kr') P(k). \quad (3.35)$$

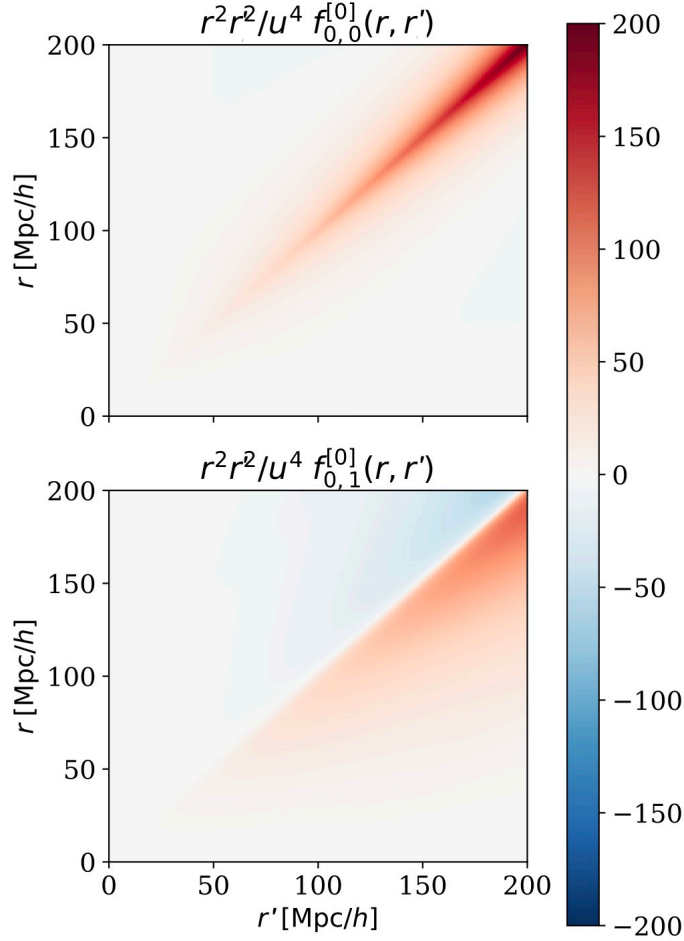


**Figure 5.** Here, we show Eq. (3.35) choosing  $n = 0$ ,  $\ell = 0$ , and  $\ell' = \{0, 1\}$ . The plot has been taken from section 3 of [13]. The *upper panel* shows the integral for  $\ell' = 0$  and is largest along the diagonal. The *lower panel* shows the integral for  $\ell' = 1$  and is largest in the off-diagonal elements. Since the 4PCF can be approximated as the square of the 2PCF on large scales,  $(\xi_0)^2(r) \sim (1/r^2)^2$ , we have weighted the integral by  $r^2 r_i^2 / u^4$ , with  $u \equiv 10$  [Mpc/h], to take out its fall-off.

After evaluation of the  $\widehat{\mathbf{s}}$  integral using Eq. (C.22), we find:

$$\begin{aligned}
\text{Cov}_{4,1\text{L}}^{[2],\text{PC-P-S}}(\mathbf{R}, \mathbf{R}') &= \sum_{\text{All}} c_{j,n}^{(\mu)} c_{j',n'}^{(\beta)} \overline{\mathcal{Q}}_{(\text{PC-P-S})}^{\Lambda, \Lambda'} \\
&\times w_{L_{k_1}, L_{10}} \widehat{G}_{L_{10}, L_{10}, j} w_{L_{k_2}, L_{20}} \widehat{G}_{L_{20}, L_{20}, j} \\
&\times w_{L'_{k'_1}, L'_{10}} \widehat{G}_{L'_{10}, L'_{10}, j'} w_{L_{k_1}, L_{10}} \widehat{G}_{L_{10}, L_{10}, j} \\
&\times C_{L_3, L_{3s}, L'_3} \Upsilon_{L_3, L_{3s}, L'_3} \mathcal{G}_{L_3, L_{3s}, L'_3} \delta_{L_{3s}, 0}^{\text{K}} \delta_{L_3, L'_3}^{\text{K}} \\
&\times f_{L_{10}, L_{10}}^{[-n]}(r_0, r_1) f_{L'_{10}, L'_{10}}^{[-n']}(r'_0, r'_1) \\
&\times f_{L_{20}, L_{20}}^{[n]}(r_0, r_2) f_{L'_{20}, L'_{20}}^{[n']}(r'_0, r'_2) \\
&\times S_{L_3, L'_3}^{(L_{3s})}(\text{PC-P-S})(r_3, r'_3) \mathcal{P}_{\Lambda}(\widehat{\mathbf{R}}) \mathcal{P}_{\Lambda'}(\widehat{\mathbf{R}}'), \tag{3.36}
\end{aligned}$$

where the  $\Lambda$ ,  $\Lambda_s$  and  $\Lambda'$  momenta have been defined in §C.4. Table 1 provides the equation where all the constants have been defined. We have defined the radial integral  $S$  as:

$$S_{L_3, L'_3}^{(L_{3s})}(\text{PC-P-S})(r_3, r'_3) \equiv \int ds s^2 g_{L_3, L_{3s}, L'_3}^{[0]}(r_3, s, r'_3). \tag{3.37}$$

The subscripts  $L_3, L'_3$  denote the set of all angular momentum indices that affect the resulting variables (*i.e.*, the  $r_3, r'_3$  variables). The superscript  $L_{3s}$  denotes the angular momentum index that couples to  $s$  in the spherical Bessel function within the  $g$  radial integral.

### 3.2.2 PC-Half-Half Configuration

We finish with the analysis of the PC-half-half configuration as shown in Fig. 4. Using Wick's theorem for the PC-half-half configuration on Eq. (2.9) results in:

$$\begin{aligned}
\text{Cov}_{4,1\text{L}}^{[2],\text{PC-H-H}}(\mathbf{R}, \mathbf{R}') &= \prod_{v=0}^3 \int_{\mathbf{s}} \int_{\mathbf{k}_v} \int_{\mathbf{k}'_v} \left[ e^{-i\mathbf{k}_v \cdot (\mathbf{x} + \mathbf{r}_v)} e^{-i\mathbf{k}'_v \cdot (\mathbf{x} + \mathbf{r}'_v + \mathbf{s})} \right] \\
&\times \int d^3 \mathbf{q}_1 \int d^3 \mathbf{q}_2 \int d^3 \mathbf{q}'_1 \int d^3 \mathbf{q}'_2 W^{(2)}(\mathbf{q}_1, \mathbf{q}_2) \\
&\times W^{(2)}(\mathbf{q}'_1, \mathbf{q}'_2) \delta_{\text{D}}^{[3]}(\mathbf{k}_0 - \mathbf{q}_1 - \mathbf{q}_2) \delta_{\text{D}}^{[3]}(\mathbf{k}'_0 - \mathbf{q}'_1 - \mathbf{q}'_2) \\
&\times \langle \widetilde{\delta}_{\text{lin.}}(\mathbf{q}_1) \widetilde{\delta}_{\text{lin.}}(\mathbf{k}_1) \rangle \langle \widetilde{\delta}_{\text{lin.}}(\mathbf{q}_2) \widetilde{\delta}_{\text{lin.}}(\mathbf{q}'_2) \rangle \langle \widetilde{\delta}_{\text{lin.}}(\mathbf{q}'_1) \widetilde{\delta}_{\text{lin.}}(\mathbf{k}'_1) \rangle \\
&\times \langle \widetilde{\delta}_{\text{lin.}}(\mathbf{k}_2) \widetilde{\delta}_{\text{lin.}}(\mathbf{k}'_2) \rangle \langle \widetilde{\delta}_{\text{lin.}}(\mathbf{k}_3) \widetilde{\delta}_{\text{lin.}}(\mathbf{k}'_3) \rangle + 35 \text{ perm.}, \tag{3.38}
\end{aligned}$$

where 35 perm. indicates the other 35 combinations<sup>6</sup> of Wick's theorem that we can obtain for this structure. For brevity, we leave this out, but it is implicitly included in our calculations.

<sup>6</sup>Finding the number of permutations is done in four steps: i) choose one of the second-order densities in any of the two tetrahedra, then pair this second-order density with any linear densities from the same tetrahedron; one has 3 possibilities. ii) Pair the remaining second-order density with any of the second-order densities in the other tetrahedron; one has 2 possibilities. iii) with the remaining second-order density in the other tetrahedron Repeat i); one has 3 possibilities. iv) choose one of the linear densities in any of the two tetrahedra, then pair this density with a linear density in the other tetrahedron; one has 2 possibilities. Total number of permutations =  $3 \times 2 \times 3 \times 2 = 36$  perms.

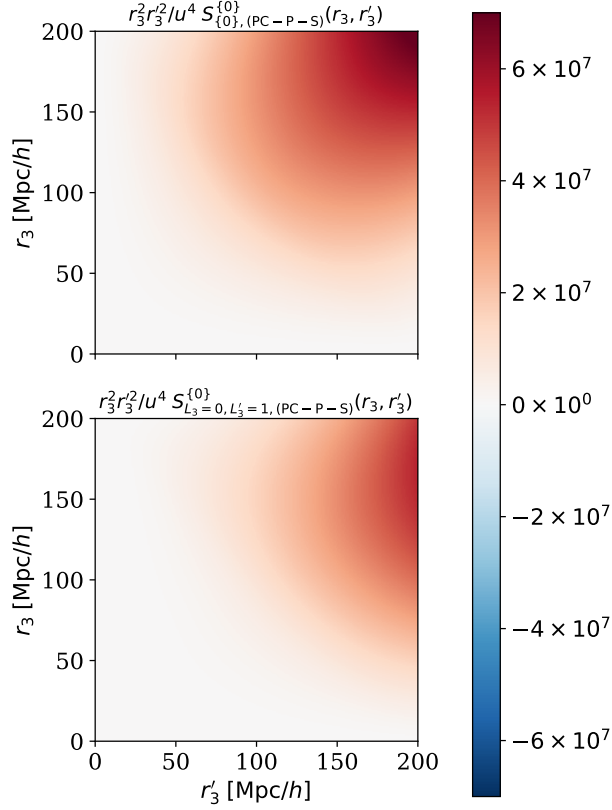


**Figure 6.** Here, we show Eq. (3.37) choosing  $n = 0$ ,  $L_3 = 0$ , and  $L'_3 = \{0, 1\}$ . The *upper panel* shows the integral for  $L'_3 = 0$ , while the *lower panel* shows the integral for  $L'_3 = 1$ . Since the 4PCF can be approximated as the square of the 2PCF on large scales,  $(\xi_0)^2(r) \sim (1/r^2)^2$ , we have weighted the integral by  $r^2 r'^2 / u^4$ , with  $u \equiv 10$  [Mpc/h], to take out its fall-off. The  $S$  integral is composed of the intermediate radial integrals,  $g$ , which reveals a rectangular boundary as shown in Fig. 2. The integration of the different rectangular boundaries creates the oval-shaped regions shown in both panels. Analytical results for similar radial integral with the power spectrum using a power law have been obtained in [13].

Evaluating the ensemble averages as power spectra and performing the integrals the  $\mathbf{q}_s$  (except for  $\mathbf{q}_2$ ),  $\mathbf{q}'_s$ ,  $\mathbf{k}_0$ ,  $\mathbf{k}'_0$ ,  $\mathbf{k}_2$  and  $\mathbf{k}_3$  by taking advantage of the Dirac delta functions, we obtain:

$$\begin{aligned}
\text{Cov}_{4,1\text{L}}^{[2],\text{PC-H-H}}(\mathbf{R}, \mathbf{R}') &= \int_{\mathbf{s}} I^{(2)}(\mathbf{r}_2, -\mathbf{s}, -\mathbf{r}'_2) I^{(3)}(\mathbf{r}_3, -\mathbf{s}, -\mathbf{r}'_3) \\
&\times \int_{\mathbf{q}_2} e^{-i\mathbf{q}_2 \cdot (\mathbf{r}_0 - \mathbf{s} - \mathbf{r}'_0)} P_{\text{lin}}(q_2) \\
&\times \int_{\mathbf{k}_1} W^{(2)}(-\mathbf{k}_1, \mathbf{q}_2) P_{\text{lin}}(k_1) e^{-i\mathbf{k}_1 \cdot (\mathbf{r}_1 - \mathbf{r}_0)} \\
&\times \int_{\mathbf{k}'_1} W^{(2)}(\mathbf{k}'_1, \mathbf{q}_2) P_{\text{lin}}(k'_1) e^{-i\mathbf{k}'_1 \cdot (\mathbf{r}'_1 - \mathbf{r}'_0)}, \tag{3.39}
\end{aligned}$$

where we have used the same definition of Eq. (3.13) on  $I^{(2)}$  and  $I^{(3)}$ ; we changed the number in parentheses from  $1 \rightarrow 2$  and  $1 \rightarrow 3$  to represent the result from the integrals of  $\mathbf{k}_2$  and  $\mathbf{k}_3$ .

We obtain the result of the remaining three integrals by expanding the exponential using Eq. (D.6), and the second-order kernel with Eq. (A.7):

$$I_{j,n}^{(1)}(\mathbf{r}_0, \mathbf{r}_2) = (4\pi)(-1)^j \sum_{L_{k_1}, L_{10}} w_{L_{k_1}, L_{10}} \widehat{G}_{L_{10}, L_{10}, j} f_{L_{10}, L_{10}}^{[n]}(r_0, r_1) \mathcal{P}_{L_{10}}(\widehat{\mathbf{r}}_0, \widehat{\mathbf{r}}_1), \quad (3.40)$$

$$I_{j',n'}^{(1p)}(\mathbf{r}'_0, \mathbf{r}'_2) = (4\pi) \sum_{L'_{k_1}, L'_{10}} w_{L'_{k_1}, L'_{10}} \widehat{G}_{L'_{10}, L'_{10}, j'} f_{L'_{10}, L'_{10}}^{[n']}(r'_0, r'_1) \mathcal{P}_{L'_{10}}(\widehat{\mathbf{r}}'_0, \widehat{\mathbf{r}}'_1), \quad (3.41)$$

$$\begin{aligned} I_{j,j',n,n'}^{(q_2)}(\mathbf{r}_0, \mathbf{r}_1) &= (4\pi)^2 \sum_{L_{q20}, L_{q2s}, L'_{q20}} C_{L_{q20}, L_{q2s}, L'_{q20}} \Upsilon_{L_{q20}, L_{q2s}, L'_{q20}} \mathcal{J}_{L_{q20}, L_{q2s}, L'_{q20}, j, j'} \\ &\times g_{L_{q20}, L_{q2s}, L'_{q20}}^{[-n-n']}(r_0, s, r'_0) \mathcal{P}_{L_{q20}, L_{q2s}, L'_{q20}}(\widehat{\mathbf{r}}_0, -\widehat{\mathbf{s}}, -\widehat{\mathbf{r}}'_0). \end{aligned} \quad (3.42)$$

After evaluation of the  $\widehat{\mathbf{s}}$  integral using Eq. (C.23), we find:

$$\begin{aligned} \text{Cov}_{4,1\text{L}}^{[2], \text{PC-H-H}}(\mathbf{R}, \mathbf{R}') &= \sum_{\text{All}} c_{j,n}^{(\mu)} c_{j',n'}^{(\beta)} \overline{\mathcal{Q}}_{(\text{PC-H-H})}^{\Lambda, \Lambda'} \\ &\times w_{L_{k_1}, L_{10}} \widehat{G}_{L_{10}, L_{10}, j} w_{L'_{k_1}, L'_{10}} \widehat{G}_{L'_{10}, L'_{10}, j'} \\ &\times C_{L_{q20}, L_{q2s}, L'_{q20}} \Upsilon_{L_{q20}, L_{q2s}, L'_{q20}} \mathcal{J}_{L_{q20}, L_{q2s}, L'_{q20}, j, j'} \\ &\times C_{L_2, L_{2s}, L'_2} \Upsilon_{L_2, L_{2s}, L'_2} \mathcal{G}_{L_2, L_{2s}, L'_2} \\ &\times C_{L_3, L_{3s}, L'_3} \Upsilon_{L_3, L_{3s}, L'_3} \mathcal{G}_{L_3, L_{3s}, L'_3} \\ &\times f_{L_{10}, L_{10}}^{[n]}(r_0, r_1) f_{L'_{10}, L'_{10}}^{[n']}(r'_0, r'_1) \\ &\times S_{\{L\}, (\text{PC-H-H})}^{\{\{L_{is}\}\}}(r_0, r'_0, r_2, r'_2, r_3, r'_3) \mathcal{P}_{\Lambda}(\widehat{\mathbf{R}}) \mathcal{P}_{\Lambda'}(\widehat{\mathbf{R}}'), \end{aligned} \quad (3.43)$$

where the  $\Lambda$ ,  $\Lambda_s$  and  $\Lambda'$  momenta have been defined in §C.5. Table 1 provides the equation where all the constants have been defined. We have defined the radial integral  $S$  as:

$$\begin{aligned} S_{\{L\}, (\text{PC-H-H})}^{\{\{L_{is}\}\}}(r_0, r'_0, r_2, r'_2, r_3, r'_3) &\equiv \int ds s^2 g_{L_{q20}, L_{q2s}, L'_{q20}}^{[-n-n']}(r_0, s, r'_0) \\ &\times g_{L_2, L_{2s}, L'_2}^{[0]}(r_2, s, r'_2) g_{L_3, L_{3s}, L'_3}^{[0]}(r_3, s, r'_3). \end{aligned} \quad (3.44)$$

The subscript  $\{L\}$  denotes the set of all angular momentum indices that affect one of the resulting variables (*i.e.*, the  $r_0, r'_0, \dots$  variables). The superscript  $(\{L_{is}\})$  denotes the set of all angular momentum indices that are coupled to  $s$  in the spherical Bessel functions.

## 4 Discussion and Conclusion

In this work, we have developed a systematic framework to compute the covariance of the 4PCF beyond the Gaussian approximation using the second-order density contrast and galaxy biasing. The key step was to generalize all second-order kernels into a single effective kernel,

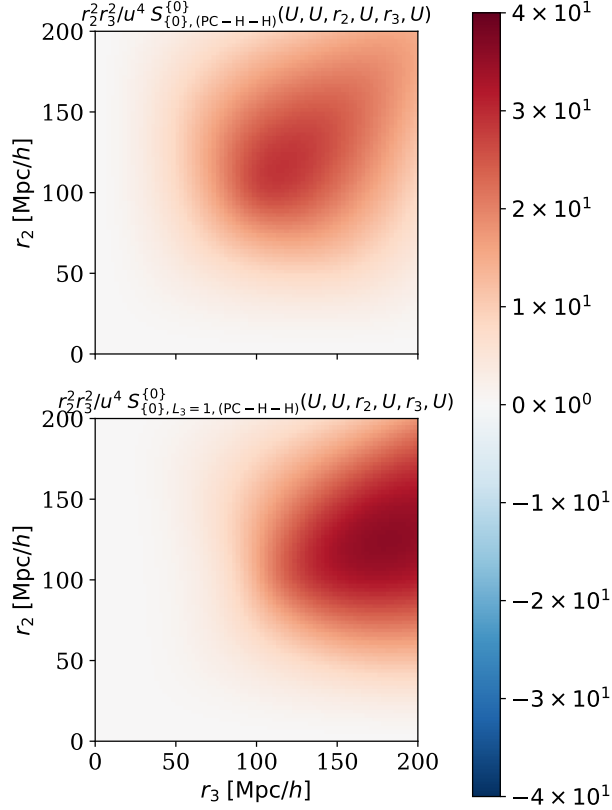


**Figure 7.** Here, we show Eq. (3.44) choosing  $n = n' = 0$  and all angular momenta  $\{L\} = 0$  except  $L_3 = \{0, 1\}$ . The *upper panel* shows the integral for  $L_3 = 0$ , while the *lower panel* shows the integral for  $L_3 = 1$ . Since the 4PCF can be approximated as the square of the 2PCF on large scales,  $(\xi_0)^2(r) \sim (1/r^2)^2$ , we have weighted the integral by  $r^2 r'^2 / u^4$ , with  $u \equiv 10$  [Mpc/h], to take out its fall-off. The  $S$  integral is composed of the intermediate radial integrals,  $g$ , which reveals a rectangular boundary as shown in Fig. 2. The integration of the different rectangular boundaries creates the oval-shaped regions shown in both panels. Analytical results for similar radial integral with the power spectrum using a power law have been obtained in [13].

which we denoted by  $W^{(2)}$  and defined in Eq. (A.7). This compact representation allows us to treat the second-order contributions in a unified way, without committing to a specific perturbative kernel.

To evaluate the loop contributions, we applied Wick's theorem to the density contrasts and organized the possible contractions into a finite set of configurations. These naturally separate into two categories: fully-connected and partially-connected. The fully-connected class (three configurations) corresponds to cases where every density contrast from one tetrahedron is paired with a density contrast from the other tetrahedron. By contrast, the partially-connected class (two configurations) always contains at least one internal loop within each tetrahedron, meaning that two densities from the same tetrahedron are contracted with each other. The explicit results for the fully-connected cases are presented in Eqs. (3.14), (3.21), and (3.27), while those for the partially-connected cases are given in Eqs. (3.36) and (3.43).

The corresponding configurations are illustrated in Figs. 1 and 4.

The practical implication of this classification is that the complete expression for the 4PCF covariance due to second-order densities can now be obtained in a straightforward manner; we compute the 4PCF covariance due to second-order densities in [14]. One starts from the general expression in Eq. (2.6), applies Wick’s theorem to all density contrasts, and then maps each contraction to one of the five configurations we have identified. Finally, by rewriting the result in terms of the generalized kernel  $W^{(2)}$ , one can substitute the specific second-order kernel relevant to their analysis.

Our formulation thus provides a clear roadmap: reduce the covariance problem to five universal building blocks, evaluate them once, and then assemble the complete answer by matching contractions to these templates. This not only streamlines the computation but also makes the framework broadly applicable to different perturbative models.

Looking ahead, an important next step will be to extend this framework to include redshift-space distortions, which are crucial for realistic galaxy surveys. In parallel, we plan to perform numerical validations against  $N$ -body simulations and mock catalogs to assess the accuracy and domain of validity of our perturbative treatment. These developments will allow us to provide survey-ready covariance matrices for upcoming data releases from DESI and beyond.

## Acknowledgments

We thank the Slepian research group for useful discussions and comments on this work. ZS especially thanks Bob Cahn for useful discussions. This publication was made possible through the support of Grant 63041 from the John Templeton Foundation. The opinions expressed in this publication are those of the author(s) and do not necessarily reflect the views of the John Templeton Foundation. ZS acknowledges funding from NASA grant number 80NSSC24M0021 and funding from UF Research AI award #00133699.

## A Generalizing the Second-Order Density Contrasts for Use in the Covariance Matrix

In this section we generalize  $\delta^{(2)}$ ,  $\delta_{\text{lin.}}^2$  and  $S^{(2)}$  to a single second-order density contrast in Fourier space. We do so using a generalized second-order kernel we term  $W^{(2)}$ , defined in Eq. (A.7).

### A.1 Second-Order Density Kernel

We begin by expressing the second-order density contrast using its inverse Fourier transform:

$$\begin{aligned}
\delta^{(2)}(\mathbf{x} + \mathbf{r}_i) &= \int \frac{d^3 \mathbf{k}_i}{(2\pi)^3} e^{-i\mathbf{k}_i \cdot (\mathbf{x} + \mathbf{r}_i)} \tilde{\delta}^{(2)}(\mathbf{k}_i) \\
&= \int \frac{d^3 \mathbf{k}_i}{(2\pi)^3} e^{-i\mathbf{k}_i \cdot (\mathbf{x} + \mathbf{r}_i)} \int d^3 \mathbf{q}_1 d^3 \mathbf{q}_2 \delta_{\text{D}}^{[3]}(\mathbf{k}_i - \mathbf{q}_1 - \mathbf{q}_2) \\
&\quad \times F^{(2)}(\mathbf{q}_1, \mathbf{q}_2) \tilde{\delta}_{\text{lin.}}(\mathbf{q}_1) \tilde{\delta}_{\text{lin.}}(\mathbf{q}_2) \\
&= \int d^3 \mathbf{q}_1 d^3 \mathbf{q}_2 e^{-i(\mathbf{q}_1 + \mathbf{q}_2) \cdot (\mathbf{x} + \mathbf{r}_i)} F^{(2)}(\mathbf{q}_1, \mathbf{q}_2) \tilde{\delta}_{\text{lin.}}(\mathbf{q}_1) \tilde{\delta}_{\text{lin.}}(\mathbf{q}_2). \tag{A.1}
\end{aligned}$$

To obtain the second equality, we used the definition of the second-order density contrast in terms of the symmetrized second-order kernel  $F^{(2)}$  [1]. To obtain the third equality, we evaluated the Dirac delta function to perform the  $\mathbf{k}_i$  integral.  $F^{(2)}$  is defined as [11, 13]:

$$\begin{aligned} F^{(2)}(\mathbf{k}_2, \mathbf{k}_3) &= \frac{17}{21} \mathcal{L}_0(\hat{\mathbf{k}}_2 \cdot \hat{\mathbf{k}}_3) + \frac{1}{2} \left( \frac{k_2}{k_3} + \frac{k_3}{k_2} \right) \mathcal{L}_1(\hat{\mathbf{k}}_2 \cdot \hat{\mathbf{k}}_3) + \frac{4}{21} \mathcal{L}_2(\hat{\mathbf{k}}_2 \cdot \hat{\mathbf{k}}_3) \\ &= 4\pi \sum_{j=0}^2 \sum_{n=-1}^1 c_{j,n}^{(F)} \mathcal{P}_j(\hat{\mathbf{k}}_2, \hat{\mathbf{k}}_3) k_2^n k_3^{-n}. \end{aligned} \quad (\text{A.2})$$

In the first line,  $\mathcal{L}_\ell$  refers to the Legendre polynomial of order  $\ell$ . In the last equality we have expressed the kernel in terms of the isotropic basis functions as already derived in [13]. The values of  $c_{j,n}^{(F)}$  are  $c_{0,0}^{(F)} = 17/21$ ,  $c_{1,1}^{(F)} = c_{1,-1}^{(F)} = -\sqrt{3}/2$ , and  $c_{2,0}^{(F)} = 4\sqrt{5}/21$ ; the rest of constants are zero.

## A.2 Squared Linear Density Contrast

We will now show that  $\tilde{\delta}_{\text{lin.}}^2$  and  $S^{(2)}$  can be expressed in the same form but with different coefficients. We first proceed with  $\tilde{\delta}_{\text{lin.}}^2$ :

$$\begin{aligned} \delta_{\text{lin.}}^2(\mathbf{x} + \mathbf{r}_i) &= \delta_{\text{lin.}}(\mathbf{x} + \mathbf{r}_i) \delta_{\text{lin.}}(\mathbf{x} + \mathbf{r}_i) \\ &= \int \frac{d^3 \mathbf{k}_i}{(2\pi)^3} e^{-i\mathbf{k}_i \cdot (\mathbf{x} + \mathbf{r}_i)} \tilde{\delta}_{\text{lin.}}(\mathbf{k}_i) \int \frac{d^3 \mathbf{k}_i''}{(2\pi)^3} e^{-i\mathbf{k}_i'' \cdot (\mathbf{x} + \mathbf{r}_i)} \tilde{\delta}_{\text{lin.}}(\mathbf{k}_i'') \\ &= \int \frac{d^3 \mathbf{k}_i}{(2\pi)^3} \frac{d^3 \mathbf{k}_i''}{(2\pi)^3} e^{-i(\mathbf{k}_i + \mathbf{k}_i'') \cdot (\mathbf{x} + \mathbf{r}_i)} \tilde{\delta}_{\text{lin.}}(\mathbf{k}_i) \tilde{\delta}_{\text{lin.}}(\mathbf{k}_i'') \\ &= (2\pi)^6 \lim_{F^{(2)} \rightarrow 1} \delta^{(2)}(\mathbf{x} + \mathbf{r}_0). \end{aligned} \quad (\text{A.3})$$

In the third equality, we observed that the linear density squared is simply what would result if we took the limit that  $F^{(2)} \rightarrow 1$  in our usual computation of the second-order density by comparing with Eq. (A.1).

## A.3 Tidal Tensor Kernel

Continuing with the tidal-tensor kernel, we find in Fourier space:

$$\begin{aligned} S^{(2)}(\mathbf{x} + \mathbf{r}_i) &= \int \frac{d^3 \mathbf{k}_i}{(2\pi)^3} e^{-i\mathbf{k}_i \cdot (\mathbf{x} + \mathbf{r}_i)} \int d^3 \mathbf{q}_1 d^3 \mathbf{q}_2 \delta_D^{[3]}(\mathbf{k}_i - \mathbf{q}_1 - \mathbf{q}_2) \\ &\quad \times S^{(2)}(\mathbf{q}_1, \mathbf{q}_2) \tilde{\delta}_{\text{lin.}}(\mathbf{q}_1) \tilde{\delta}_{\text{lin.}}(\mathbf{q}_2) \\ &= \lim_{F^{(2)} \rightarrow 2/3 \mathcal{L}_2(\mathbf{q}_1, \mathbf{q}_2)} \delta^{(2)}(\mathbf{x} + \mathbf{r}_i), \end{aligned} \quad (\text{A.4})$$

with:

$$S^{(2)}(\mathbf{q}_1, \mathbf{q}_2) = \frac{(\mathbf{q}_1 \cdot \mathbf{q}_2)^2}{q_1^2 q_2^2} - \frac{1}{3} = \frac{2}{3} \mathcal{L}_2(\hat{\mathbf{q}}_1 \cdot \hat{\mathbf{q}}_2). \quad (\text{A.5})$$

In Eq. A.4, we observed that the tidal tensor kernel is simply what would result if we took the limit that  $F^{(2)} \rightarrow (2/3) \mathcal{L}_2$  in our usual computation of the second-order density by comparing with Eq. (A.1).

Eqs. (A.1), (A.3), and (A.4) suggest that we can encapsulate their information in Fourier space in a single form for the second-order density contrast. We only need a new general second-order kernel that can be expressed in terms of any of these three second-order density contrasts.

#### A.4 Generalized Second-Order Density Contrast

Below, we present the generalized second-order density contrast and kernel:

$$\begin{aligned} \delta_\mu^{(2)}(\mathbf{x} + \mathbf{r}_0) &= \int \frac{d^3 \mathbf{k}_0}{(2\pi)^3} e^{-i\mathbf{k}_0 \cdot (\mathbf{x} + \mathbf{r}_0)} \int d^3 \mathbf{q}_1 d^3 \mathbf{q}_2 \delta_D^{[3]}(\mathbf{k}_0 - \mathbf{q}_1 - \mathbf{q}_2) \\ &\quad \times W_\mu^{(2)}(\mathbf{q}_1, \mathbf{q}_2) \tilde{\delta}_{\text{lin.}}(\mathbf{q}_1) \tilde{\delta}_{\text{lin.}}(\mathbf{q}_2), \end{aligned} \quad (\text{A.6})$$

with

$$\begin{aligned} W_\mu^{(2)}(\mathbf{q}_1, \mathbf{q}_2) &= 4\pi \sum_{j=0}^2 \sum_{n=-1}^1 c_{j,n}^{(\mu)} \mathcal{P}_j(\hat{\mathbf{q}}_1, \hat{\mathbf{q}}_2) q_1^n q_2^{-n} \\ &= 4\pi \sum_{j,m_j,n} c_{j,n}^{(\mu)} D_j Y_{j,m_j}(\hat{\mathbf{q}}_1) Y_{j,m_j}^*(\hat{\mathbf{q}}_2) q_1^n q_2^{-n}, \end{aligned} \quad (\text{A.7})$$

where  $\mu$  runs over  $\{0, 1, 2\}$  such that  $\{\tilde{\delta}_0^{(2)}, \tilde{\delta}_1^{(2)}, \tilde{\delta}_2^{(2)}\} = \{S^{(2)}, \tilde{\delta}^{(2)}, \tilde{\delta}_{\text{lin.}}^2\}$ . If we evaluate  $W^{(2)} = S^{(2)}$ , the only non-zero coefficient will be  $c_{j,n}^{(\mu)} = c_{2,0}^{(0)} = 2(\sqrt{5}/3)$ . If  $W^{(2)} = \tilde{\delta}_{\text{lin.}}^2$ , the only non-zero coefficient will be  $c_{j,n}^{(\mu)} = c_{0,0}^{(2)} = 1$ . When  $W^{(2)} = \delta^{(2)}$  the non-zero coefficients are  $c_{0,0}^{(F)} = 17/21$ ,  $c_{1,1}^{(F)} = c_{1,-1}^{(F)} = -\sqrt{3}/2$ , and  $c_{2,0}^{(F)} = 4\sqrt{5}/21$  [13]. In the second equality above we have defined  $D_j \equiv (-1)^j / \sqrt{2j+1}$  [3].

## B Evaluation of the Angular Integrals for the Covariance with Second-Order Densities

In this section we show the evaluation of the main angular integrals in this work. We start with the evaluation of one 3-argument isotropic basis function when all its arguments are the same:

$$\begin{aligned} \mathcal{G}_{L_1, L_2, L_3} &\equiv \int_{\hat{\mathbf{k}}} \mathcal{P}_{L_1, L_2, L_3}(\hat{\mathbf{k}}, \hat{\mathbf{k}}, \hat{\mathbf{k}}) \\ &= (-1)^{L_1+L_2+L_3} \sum_{M_1, M_2, M_3} \begin{pmatrix} L_1 & L_2 & L_3 \\ M_1 & M_2 & M_3 \end{pmatrix} \int_{\hat{\mathbf{k}}} Y_{L_1, M_1}(\hat{\mathbf{k}}) Y_{L_2, M_2}(\hat{\mathbf{k}}) Y_{L_3, M_3}(\hat{\mathbf{k}}) \\ &= (-1)^{L_1+L_2+L_3} \left( \frac{(2L_1+1)(2L_2+1)(2L_3+1)}{4\pi} \right)^{1/2} \begin{pmatrix} L_1 & L_2 & L_3 \\ 0 & 0 & 0 \end{pmatrix} \sum_{M_1, M_2, M_3} \begin{pmatrix} L_1 & L_2 & L_3 \\ M_1 & M_2 & M_3 \end{pmatrix}^2 \\ &= \left( \frac{(2L_1+1)(2L_2+1)(2L_3+1)}{4\pi} \right)^{1/2} \begin{pmatrix} L_1 & L_2 & L_3 \\ 0 & 0 & 0 \end{pmatrix}. \end{aligned} \quad (\text{B.1})$$

In the second equality, we have expanded the 3-argument isotropic basis function using its definition:

$$\begin{aligned} \mathcal{P}_{L, L', L''}(\hat{\mathbf{k}}, \hat{\mathbf{k}}, \hat{\mathbf{k}}) &= (-1)^{L+L'+L''} \sum_{M, M', M''} \begin{pmatrix} L & L' & L'' \\ M & M' & M'' \end{pmatrix} \\ &\quad \times \int_{\hat{\mathbf{k}}} Y_{L, M}(\hat{\mathbf{k}}) Y_{L', M'}(\hat{\mathbf{k}}) Y_{L'', M''}(\hat{\mathbf{k}}). \end{aligned} \quad (\text{B.2})$$

In the third equality, we used the Gaunt integral of three spherical harmonics, given by [7] in their Eq. (34.3.22):

$$G_{M_1, M_2, M_3}^{L_1, L_2, L_3} \equiv \left( \frac{(2L_1 + 1)(2L_2 + 1)(2L_3 + 1)}{4\pi} \right)^{1/2} \begin{pmatrix} L_1 & L_2 & L_3 \\ 0 & 0 & 0 \end{pmatrix} \begin{pmatrix} L_1 & L_2 & L_3 \\ M_1 & M_2 & M_3 \end{pmatrix}, \quad (\text{B.3})$$

and in the fourth equality we used Eq. (34.3.18) in [7], and dropped the negative sign since the  $3j$  symbol imposes an even sum of  $L_1$ ,  $L_2$  and  $L_3$ .

Next, we compute the integral over one 2-argument isotropic basis function times two spherical harmonics with its arguments the same. We expand the isotropic function into spherical harmonics and obtain:

$$\begin{aligned} \hat{G}_{L, L, \ell} &\equiv \sum_m \int_{\hat{\mathbf{k}}} \mathcal{P}_L(\hat{\mathbf{k}}, \hat{\mathbf{k}}) Y_{\ell, m}(\hat{\mathbf{k}}) \\ &= D_L \sum_{M, m} G_{M, M, m}^{L, L, \ell}, \end{aligned} \quad (\text{B.4})$$

with  $D_L$  defined below Eq. (A.7). Next, we evaluate the integral of one 3-argument isotropic basis function, with all its arguments being the same, against one spherical harmonic of the same argument:

$$\begin{aligned} \mathcal{H}_{L, L', L'', \ell} &\equiv \sum_m \int_{\hat{\mathbf{k}}} \mathcal{P}_{L, L', L''}(\hat{\mathbf{k}}, \hat{\mathbf{k}}, \hat{\mathbf{k}}) Y_{\ell, m}(\hat{\mathbf{k}}) \\ &= (-1)^{L+L'+L''} \sum_{M, M', M'', m} \begin{pmatrix} L & L' & L'' \\ M & M' & M'' \end{pmatrix} \\ &\quad \times \int_{\hat{\mathbf{k}}} Y_{L, M}(\hat{\mathbf{k}}) Y_{L', M'}(\hat{\mathbf{k}}) Y_{L'', M''}(\hat{\mathbf{k}}) Y_{\ell, m}(\hat{\mathbf{k}}) \\ &= (-1)^{L+L'+L''} \sum_{M, M', M'', m} \sum_{\ell', m'} \begin{pmatrix} L & L' & L'' \\ M & M' & M'' \end{pmatrix} \\ &\quad \times G_{L'', \ell', \ell'}^{M'', -m'} G_{L, L', \ell'}^{M, M', m'}. \end{aligned} \quad (\text{B.5})$$

To obtain the result in third equality, we first combined a product of two spherical harmonics into a sum over single one, and then evaluated the integral of a product of three spherical harmonics as defined in Eq. (B.3).

Last, we evaluate the integral of a product of one 3-argument isotropic basis function

whose arguments are all the same against two spherical harmonics:

$$\begin{aligned}
\mathcal{J}_{L,L',L'',\ell,\ell''} &\equiv \sum_{m,m'} \int_{\hat{\mathbf{k}}} \mathcal{P}_{L,L',L''}(\hat{\mathbf{k}}, \hat{\mathbf{k}}, \hat{\mathbf{k}}) Y_{\ell,m}(\hat{\mathbf{k}}) Y_{\ell',m'}(\hat{\mathbf{k}}) \\
&= (-1)^{L+L'+L''} \sum_{M,M',M'',m,m'} \begin{pmatrix} L & L' & L'' \\ M & M' & M'' \end{pmatrix} \\
&\quad \times \int_{\hat{\mathbf{k}}} Y_{L,M}(\hat{\mathbf{k}}) Y_{L',M'}(\hat{\mathbf{k}}) Y_{L'',M''}(\hat{\mathbf{k}}) Y_{\ell,m}(\hat{\mathbf{k}}) Y_{\ell',m'}(\hat{\mathbf{k}}) \\
&= (-1)^{L+L'+L''} \sum_{M,M',M'',m,m'} \sum_{\ell'',m''} \sum_{\ell''',m'''} \begin{pmatrix} L & L' & L'' \\ M & M' & M'' \end{pmatrix} \\
&\quad \times G_{L'',\ell,\ell''}^{M'',m,-m''} G_{\ell',\ell'',\ell'''}^{m',m'',-m'''} G_{L,L',\ell'''}^{M,M',m'''} .
\end{aligned} \tag{B.6}$$

Here, we have followed the same steps as in Eq. (B.5), with the exception that, to reach the third equality, we needed to combine two spherical harmonics into a single one twice in order to obtain an integral over a product of three spherical harmonics.

## C Evaluation of $\hat{\mathbf{s}}$ Integrals

In this section, we evaluate the  $\hat{\mathbf{s}}$  integrals of the five configurations that contribute to the 1-loop covariance in §2, following [3, 8] by averaging the isotropic basis over rotations  $R$ ,  $R'$ , and  $S$ . Averaging over rotations  $R$  and  $R'$  enables to express the angular dependence in terms of a single isotropic basis function, while averaging over rotation  $S$  enables the evaluation of the  $\hat{\mathbf{s}}$  dependence as previously demonstrated in [3, 8].

### C.1 $\hat{\mathbf{s}}$ Integral for the Primary-Secondary Configuration

We begin our analysis of these integrals with the Primary-Secondary configuration:

$$\begin{aligned}
&\int dR dR' dS \mathcal{P}_{L_1,L_{1s},L'_1}(R\hat{\mathbf{r}}_1, -S\hat{\mathbf{s}}, -R'\hat{\mathbf{r}}'_1) \mathcal{P}_{L_{30},L'_{3s},L'_3}(R\hat{\mathbf{r}}_0, S\hat{\mathbf{s}}, -R'\hat{\mathbf{r}}'_3) \\
&\quad \times \mathcal{P}_{L_{20},L'_{2s},L'_2}(R\hat{\mathbf{r}}_0, S\hat{\mathbf{s}}, -R'\hat{\mathbf{r}}'_2) \mathcal{P}_{L_3,L_{3s},L'_{30}}(R\hat{\mathbf{r}}_3, -S\hat{\mathbf{s}}, -R'\hat{\mathbf{r}}'_0) \\
&\quad \times \mathcal{P}_{L_2,L_{2s},L'_{20}}(R\hat{\mathbf{r}}_2, -S\hat{\mathbf{s}}, -R'\hat{\mathbf{r}}'_0).
\end{aligned} \tag{C.1}$$

Expanding the isotropic functions into spherical harmonics, we find:

$$\begin{aligned}
&\int dR dR' dS (-1)^{L_1+L_2+L_3+L_{20}+L_{30}} \\
&\quad \times \sum_{\text{All } M} \mathcal{C}_{M_1,M_{1s},M'_1}^{L_1,L_{1s},L'_1} \mathcal{C}_{M_{30},M'_{3s},M'_3}^{L_{30},L'_{3s},L'_3} \mathcal{C}_{M_{20},M'_{2s},M'_2}^{L_{20},L'_{2s},L'_2} \mathcal{C}_{M_2,M_{2s},M'_{20}}^{L_2,L_{2s},L'_{20}} \mathcal{C}_{M_3,M_{3s},M'_{30}}^{L_3,L_{3s},L'_{30}} \\
&\quad \times Y_{L_{20},M_{20}}(R\hat{\mathbf{r}}_0) Y_{L_{30},M_{30}}(R\hat{\mathbf{r}}_0) Y_{L_1,M_1}(R\hat{\mathbf{r}}_1) Y_{L_2,M_2}(R\hat{\mathbf{r}}_2) Y_{L_3,M_3}(R\hat{\mathbf{r}}_3) \\
&\quad \times Y_{L'_{2s},M'_{2s}}(S\hat{\mathbf{s}}) Y_{L'_{3s},M'_{3s}}(S\hat{\mathbf{s}}) Y_{L_{1s},M_{1s}}(S\hat{\mathbf{s}}) Y_{L_{2s},M_{2s}}(S\hat{\mathbf{s}}) Y_{L_{3s},M_{3s}}(S\hat{\mathbf{s}}) \\
&\quad \times Y_{L'_2,M'_2}(R'\hat{\mathbf{r}}'_2) Y_{L'_3,M'_3}(R'\hat{\mathbf{r}}'_3) Y_{L'_1,M'_1}(R'\hat{\mathbf{r}}'_1) Y_{L'_{20},M'_{20}}(R'\hat{\mathbf{r}}'_0) Y_{L'_{30},M'_{30}}(R'\hat{\mathbf{r}}'_0),
\end{aligned} \tag{C.2}$$

where we define  $\mathcal{C}$  as [8]:

$$\begin{aligned} \mathcal{C}_M^\Lambda &= (-1)^{\sum_i \Lambda_i} \sqrt{2\ell_{12} + 1} \times \cdots \times \sqrt{2\ell_{12\dots n-2} + 1} \\ &\times \sum_{m_{12}, \dots} (-1)^\kappa \begin{pmatrix} \ell_1 & \ell_2 & \ell_{12} \\ m_1 & m_2 & -m_{12} \end{pmatrix} \begin{pmatrix} \ell_{12} & \ell_3 & \ell_{123} \\ m_{12} & m_3 & -m_{123} \end{pmatrix} \cdots \\ &\times \begin{pmatrix} \ell_{12\dots n-2} & \ell_{n-1} & \ell_n \\ m_{12\dots n-2} & m_{n-1} & m_n \end{pmatrix}, \end{aligned} \quad (\text{C.3})$$

and  $\Lambda = \{\ell_1, \ell_2, (\ell_{12}), \ell_3, (\ell_{123}), \dots, \ell_n\}$  with the 'intermediate' angular momenta in brackets,  $M = \{m_1, m_2, (m_{12}), m_3, (m_{123}), \dots, m_n\}$ , and  $\kappa = \ell_{12} - m_{12} + \ell_{123} - m_{123} + \cdots + \ell_{12\dots n-2} - m_{12\dots n-2}$ .

We analyze the integrals one by one, starting with the integral over the rotational average of the  $\hat{\mathbf{S}}$  vector, for which we find:

$$\begin{aligned} &\int dS Y_{L'_{2s}, M'_{2s}}(S\hat{\mathbf{S}}) Y_{L'_{3s}, M'_{3s}}(S\hat{\mathbf{S}}) Y_{L_{1s}, M_{1s}}(S\hat{\mathbf{S}}) Y_{L_{2s}, M_{2s}}(S\hat{\mathbf{S}}) Y_{L_{3s}, M_{3s}}(S\hat{\mathbf{S}}) \\ &= \int d\hat{\mathbf{n}} Y_{L'_{2s}, M'_{2s}}(\hat{\mathbf{n}}) Y_{L'_{3s}, M'_{3s}}(\hat{\mathbf{n}}) Y_{L_{1s}, M_{1s}}(\hat{\mathbf{n}}) Y_{L_{2s}, M_{2s}}(\hat{\mathbf{n}}) Y_{L_{3s}, M_{3s}}(\hat{\mathbf{n}}) \\ &= \sum_{\ell, \ell'} \sum_{m, m'} G_{M'_{2s}, M'_{3s}, -m}^{L'_{2s}, L'_{3s}, \ell} G_{m, M_{1s}, -m'}^{\ell, L_{1s}, \ell'} G_{m', M_{2s}, M_{3s}}^{\ell', L_{2s}, L_{3s}}, \end{aligned} \quad (\text{C.4})$$

where we have defined  $\hat{\mathbf{n}} \equiv S\hat{\mathbf{S}}$  in the first equality, and solved the resulting integral in the second equality in terms of the Gaunt integrals.

Next, we evaluate the integral over the rotational average of the  $\hat{\mathbf{r}}'$  vectors, for which the solution is explicitly given in Eq. (2.31) of [3]. We state the result here:

$$\begin{aligned} &\int dR' Y_{L'_2, M'_2}(R'\hat{\mathbf{r}}'_2) Y_{L'_3, M'_3}(R'\hat{\mathbf{r}}'_3) Y_{L'_1, M'_1}(R'\hat{\mathbf{r}}'_1) Y_{L'_{20}, M'_{20}}(R'\hat{\mathbf{r}}'_0) Y_{L'_{30}, M'_{30}}(R'\hat{\mathbf{r}}'_0) \\ &= \sum_{L'_0, M'_0} G_{M'_{20}, M'_{30}, -M'_0}^{L'_{20}, L'_{30}, L'_0} \sum_{\Lambda'} \mathcal{C}_{M'}^{\Lambda'} \mathcal{P}_{\Lambda'}(\hat{\mathbf{R}}'), \end{aligned} \quad (\text{C.5})$$

where we have defined  $\Lambda' = \{L'_0, L'_1, L'_2, L'_3\}$  and likewise for  $M' = \{M'_0, M'_1, M'_2, M'_3\}$ . We have combined the two spherical harmonics of the  $\hat{\mathbf{r}}'_0$  vectors into a single one in the second equality, and used Eq. (2.31) of [3] to evaluate the resulting integral with four spherical harmonics.

Lastly, we evaluate the integral over the rotational average of the  $\hat{\mathbf{r}}$  vectors. We follow the same procedure as for the  $\hat{\mathbf{r}}'$  evaluation:

$$\begin{aligned} &\int dR' Y_{L_{20}, M_{20}}(R\hat{\mathbf{r}}_0) Y_{L_{30}, M_{30}}(R\hat{\mathbf{r}}_0) Y_{L_1, M_1}(R\hat{\mathbf{r}}_1) Y_{L_2, M_2}(R\hat{\mathbf{r}}_2) Y_{L_3, M_3}(R\hat{\mathbf{r}}_3) \\ &= \sum_{L_0, M_0} G_{M_{20}, M_{30}, -M_0}^{L_{20}, L_{30}, L_0} \sum_{\Lambda} \mathcal{C}_M^\Lambda \mathcal{P}_\Lambda(\hat{\mathbf{R}}), \end{aligned} \quad (\text{C.6})$$

where we have defined  $\Lambda = \{L_0, L_1, L_2, L_3\}$  and  $M = \{M_0, M_1, M_2, M_3\}$ .

Therefore, the result of the  $\hat{\mathbf{s}}$  integral for the primary-primary configuration can be written as:

$$\begin{aligned}
& \int dR dR' dS \mathcal{P}_{L_{20}, L_{20s}, L'_2}(R\hat{\mathbf{r}}_0, -S\hat{\mathbf{s}}, -R'\hat{\mathbf{r}}'_2) \\
& \times \mathcal{P}_{L_{30}, L_{30s}, L'_3}(R\hat{\mathbf{r}}_0, -S\hat{\mathbf{s}}, -R'\hat{\mathbf{r}}'_3) \mathcal{P}_{L_1, L_{1s}, L'_1}(R\hat{\mathbf{r}}_1, -S\hat{\mathbf{s}}, -R'\hat{\mathbf{r}}'_1) \\
& \times \mathcal{P}_{L_2, L_{2s}, L'_2}(R\hat{\mathbf{r}}_2, -S\hat{\mathbf{s}}, -R'\hat{\mathbf{r}}'_0) \mathcal{P}_{L_3, L_{3s}, L'_{30}}(R\hat{\mathbf{r}}_3, -S\hat{\mathbf{s}}, -R'\hat{\mathbf{r}}'_0) \\
& = \sum_{\Lambda, \Lambda_s, \Lambda'} \bar{\mathcal{Q}}_{(\text{P-S})}^{\Lambda, \Lambda_s, \Lambda'} \mathcal{P}_{\Lambda}(\hat{\mathbf{R}}) \mathcal{P}_{\Lambda'}(\hat{\mathbf{R}}'), \tag{C.7}
\end{aligned}$$

where we have defined  $\Lambda_s = \{L_{20s}, L_{30s}, L_{1s}, L_{2s}, L_{3s}\}$  and  $\bar{\mathcal{Q}}$  as:

$$\begin{aligned}
\bar{\mathcal{Q}}_{(\text{P-S})}^{\Lambda, \Lambda_s, \Lambda'} & \equiv (-1)^{\sum_i \Lambda_i} \sum_{\text{All M}} \mathcal{C}_{M_{20}, M_{2s}, M'_2}^{L_{20}, L_{2s}, L'_2} \mathcal{C}_{M_{30}, M_{3s}, M'_3}^{L_{30}, L_{3s}, L'_3} \mathcal{C}_{M_1, M_{1s}, M'_1}^{L_1, L_{1s}, L'_1} \mathcal{C}_{M_2, M_{2s}, M'_{20}}^{L_2, L_{2s}, L'_{20}} \mathcal{C}_{M_3, M_{3s}, M'_{30}}^{L_3, L_{3s}, L'_{30}} \\
& \times \sum_{L_0, L'_0} \sum_{M_0, M'_0} G_{M_{20}, M_{30}, -M_0}^{L_{20}, L_{30}, L_0} \mathcal{C}_M^{\Lambda} G_{M'_{20}, M'_{30}, -M'_0}^{L'_{20}, L'_{30}, L'_0} \mathcal{C}_{M'}^{\Lambda'} \\
& \times \sum_{\ell, \ell'} \sum_{m, m'} G_{M_{2s}, M_{3s}, -m}^{L_{20s}, L'_{30s}, \ell} G_{m, M_{1s}, -m'}^{\ell, L_{1s}, \ell'} G_{m', M_{2s}, M_{3s}}^{\ell', L_{2s}, L_{3s}} \tag{C.8}
\end{aligned}$$

## C.2 $\hat{\mathbf{s}}$ Integral for the Half-Half Configuration

We continue the analysis of the  $\hat{\mathbf{s}}$  integrals by evaluating the half-half configuration:

$$\begin{aligned}
& \int dR dR' dS \mathcal{P}_{L_{q0}, L'_{qs}, L'_{q0}}(-R\hat{\mathbf{r}}_0, S\hat{\mathbf{s}}, R'\hat{\mathbf{r}}'_0) \mathcal{P}_{L_{30}, L'_{3s}, L'_3}(-R\hat{\mathbf{r}}_0, S\hat{\mathbf{s}}, R'\hat{\mathbf{r}}'_3) \\
& \times \mathcal{P}_{L_1, L_{1s}, L'_1}(R\hat{\mathbf{r}}_1, -S\hat{\mathbf{s}}, -R'\hat{\mathbf{r}}'_1) \mathcal{P}_{L_2, L_{2s}, L'_2}(R\hat{\mathbf{r}}_2, -S\hat{\mathbf{s}}, -R'\hat{\mathbf{r}}'_2) \\
& \times \mathcal{P}_{L_3, L_{3s}, L'_{30}}(R\hat{\mathbf{r}}_3, -S\hat{\mathbf{s}}, -R'\hat{\mathbf{r}}'_0). \tag{C.9}
\end{aligned}$$

The result of evaluating the above integral will be analogous to the primary-secondary configuration, the only difference being that  $\Lambda_s = \{L_{qs}, L'_{3s}, L_{1s}, L_{2s}, L_{3s}\}$ , and the  $\mathcal{Q}$  constant is:

$$\begin{aligned}
\bar{\mathcal{Q}}_{(\text{H-H})}^{\Lambda, \Lambda_s, \Lambda'} & \equiv (-1)^{L_1 + L_2 + L_3 + L'_3 + L'_{3s} + L'_{q0} + L'_{qs}} \sum_{\text{All M}} \mathcal{C}_{M_{q0}, M_{qs}, M'_{q0}}^{L_{q0}, L'_{qs}, L'_{q0}} \mathcal{C}_{M_{30}, M_{3s}, M'_3}^{L_{30}, L_{3s}, L'_3} \mathcal{C}_{M_1, M_{1s}, M'_1}^{L_1, L_{1s}, L'_1} \\
& \times \mathcal{C}_{M_2, M_{2s}, M'_{20}}^{L_2, L_{2s}, L'_{20}} \mathcal{C}_{M_3, M_{3s}, M'_{30}}^{L_3, L_{3s}, L'_{30}} \sum_{L_0, L'_0} \sum_{M_0, M'_0} G_{M_{20}, M_{30}, -M_0}^{L_{20}, L_{30}, L_0} \mathcal{C}_M^{\Lambda} G_{M'_{20}, M'_{30}, -M'_0}^{L'_{20}, L'_{30}, L'_0} \mathcal{C}_{M'}^{\Lambda'} \\
& \times \sum_{\ell, \ell'} \sum_{m, m'} G_{M_{qs}, M'_{3s}, -m}^{L_{qs}, L'_{3s}, \ell} G_{m, M_{1s}, -m'}^{\ell, L_{1s}, \ell'} G_{m', M_{2s}, M_{3s}}^{\ell', L_{2s}, L_{3s}} \tag{C.10}
\end{aligned}$$

## C.3 $\hat{\mathbf{s}}$ Integral for the Primary-Primary Configuration

Next, we evaluate the primary-primary configuration  $\hat{\mathbf{s}}$  integral, given by:

$$\begin{aligned}
& \int dR dR' dS \mathcal{P}_{L_{01}, L_{1qs}, L'_{01}}(R\hat{\mathbf{r}}_0, -S\hat{\mathbf{s}}, -R'\hat{\mathbf{r}}'_0) \mathcal{P}_{L_{02}, L_{2qs}, L'_{02}}(R\hat{\mathbf{r}}_0, -S\hat{\mathbf{s}}, -R'\hat{\mathbf{r}}'_0) \\
& \times \mathcal{P}_{L_1, L_{1s}, L'_1}(R\hat{\mathbf{r}}_1, -S\hat{\mathbf{s}}, -R'\hat{\mathbf{r}}'_1) \mathcal{P}_{L_2, L'_{2s}, L'_2}(R\hat{\mathbf{r}}_2, -S\hat{\mathbf{s}}, -R'\hat{\mathbf{r}}'_2) \\
& \times \mathcal{P}_{L_3, L'_{3s}, L'_3}(R\hat{\mathbf{r}}_3, -S\hat{\mathbf{s}}, -R'\hat{\mathbf{r}}'_3). \tag{C.11}
\end{aligned}$$

Evaluating these integrals, like the half-half configuration, follows the same steps as shown in the primary-secondary configuration. Once again,  $\Lambda_s$  changes to  $\Lambda_s = \{L_{1qs}, L'_{2qs}, L_{1s}, L_{2s}, L_{3s}\}$ , and the  $\mathcal{Q}$  constant is:

$$\begin{aligned} \overline{\mathcal{Q}}_{(\text{P-P})}^{\Lambda, \Lambda_s, \Lambda'} &\equiv (-1)^{L_{01}+L_{02}+L_{11}+L'_3+L'_{3s}+L'_{q'_0}+L'_{qs}} \sum_{\text{All M}} \mathcal{C}_{M_{01}, M_{1qs}, M'_{01}}^{L_{01}, L'_{1qs}, L'_{01}} \mathcal{C}_{M_{02}, M_{2qs}, M'_{02}}^{L_{02}, L_{2qs}, L'_{02}} \mathcal{C}_{M_1, M_{1s}, M'_1}^{L_1, L_{1s}, L'_1} \\ &\times \mathcal{C}_{M_2, M_{2s}, M'_2}^{L_2, L_{2s}, L'_2} \mathcal{C}_{M_3, M_{3s}, M'_3}^{L_3, L_{3s}, L'_3} \sum_{L_0, L'_0} \sum_{M_0, M'_0} G_{M_{01}, M_{02}, -M_0}^{L_{01}, L_{02}, L_0} \mathcal{C}_M^\Lambda G_{M'_{01}, M'_{02}, -M'_0}^{L'_{01}, L'_{02}, L'_0} \mathcal{C}_{M'}^{\Lambda'} \\ &\times \sum_{\ell, \ell'} \sum_{m, m'} G_{M_{1qs}, M_{2qs}, -m}^{L_{1qs}, L'_{2qs}, \ell} G_{m, M_{1s}, -m'}^{\ell, L_{1s}, \ell'} G_{m', M_{2s}, M_{3s}}^{\ell', L_{2s}, L_{3s}}. \end{aligned} \quad (\text{C.12})$$

#### C.4 $\hat{\mathbf{s}}$ Integral for the PC-Primary-Secondary Configuration

We continue the analysis of the  $\hat{\mathbf{s}}$  integrals by evaluating the PC-primary-secondary configurations:

$$\begin{aligned} &\int dR dR' dS \mathcal{P}_{L_{10}}(R\hat{\mathbf{r}}_0, R\hat{\mathbf{r}}_1) \mathcal{P}_{L_{20}}(R\hat{\mathbf{r}}_0, R\hat{\mathbf{r}}_2) \\ &\times \mathcal{P}_{L'_{10}}(R'\hat{\mathbf{r}}'_0, R'\hat{\mathbf{r}}'_1) \mathcal{P}_{L'_{20}}(R'\hat{\mathbf{r}}'_0, R'\hat{\mathbf{r}}'_2) \mathcal{P}_{L_3, L_{3s}, L'_3}(R\hat{\mathbf{r}}_3, -S\hat{\mathbf{s}}, -R'\hat{\mathbf{r}}'_3). \end{aligned} \quad (\text{C.13})$$

Expressing the 3-argument isotropic basis function in terms of the spherical harmonics shows that the result of the  $dS$  integral gives  $L_{3s} = 0$ ; through the 3- $j$  symbol from the expansion, we then obtain  $L_3 = L'_3$ . The primed integrals can be performed to obtain:

$$\begin{aligned} &(-1)^{L_3} \int dR' Y_{L'_{10}, M'_{10}}(R'\hat{\mathbf{r}}'_0) Y_{L'_{20}, M'_{20}}(R'\hat{\mathbf{r}}'_0) Y_{L'_{10}, M'_{10}}(R'\hat{\mathbf{r}}'_1) Y_{L'_{20}, M'_{20}}(R'\hat{\mathbf{r}}'_2) Y_{L_3, M_3}(R'\hat{\mathbf{r}}'_3) \\ &= (-1)^{L_3} \sum_{L'_0, M'_0} G_{M'_{10}, M'_{20}, -M'_0}^{L'_{10}, L'_{20}, L'_0} \int dR Y_{L'_0, M'_0}(R\hat{\mathbf{r}}_0) Y_{L'_{10}, M'_{10}}(R'\hat{\mathbf{r}}'_1) Y_{L'_{20}, M'_{20}}(R'\hat{\mathbf{r}}'_2) Y_{L_3, M_3}(R'\hat{\mathbf{r}}'_3) \\ &= (-1)^{L_3} \sum_{\Lambda'} \mathcal{C}_{M'}^{\Lambda'} \mathcal{P}_{\Lambda'}(\hat{\mathbf{r}}'_0, \hat{\mathbf{r}}'_1, \hat{\mathbf{r}}'_2, \hat{\mathbf{r}}'_3) \sum_{L'_0, M'_0} G_{M'_{10}, M'_{20}, -M'_0}^{L'_{10}, L'_{20}, L'_0}, \end{aligned} \quad (\text{C.14})$$

where we have defined  $\Lambda' \equiv \{L'_0, L'_{10}, L'_{20}, L_3\}$ . Following the same steps, we evaluate the unprimed integrals and find:

$$\begin{aligned} &\int dR Y_{L_{10}, M_{10}}(R\hat{\mathbf{r}}_0) Y_{L_{20}, M_{20}}(R\hat{\mathbf{r}}_0) Y_{L_{10}, M_{10}}(R\hat{\mathbf{r}}_1) Y_{L_{20}, M_{20}}(R\hat{\mathbf{r}}_2) Y_{L_3, M_3}(R\hat{\mathbf{r}}_3) \\ &= \sum_{\Lambda} \mathcal{C}_M^\Lambda \mathcal{P}_\Lambda(\hat{\mathbf{r}}_0, \hat{\mathbf{r}}_1, \hat{\mathbf{r}}_2, \hat{\mathbf{r}}_3) \sum_{L_0, M_0} G_{M_{10}, M_{20}, -M_0}^{L_{10}, L_{20}, L_0}, \end{aligned} \quad (\text{C.15})$$

where we have defined  $\Lambda \equiv \{L_0, L_{10}, L_{20}, L_3\}$ . Therefore, the result of evaluating the  $\hat{\mathbf{s}}$  by means of averaging over all rotations results in:

$$\begin{aligned} &\int dR dR' dS \mathcal{P}_{L_{10}}(R\hat{\mathbf{r}}_0, R\hat{\mathbf{r}}_1) \mathcal{P}_{L_{20}}(R\hat{\mathbf{r}}_0, R\hat{\mathbf{r}}_2) \\ &\times \mathcal{P}_{L'_{10}}(R'\hat{\mathbf{r}}'_0, R'\hat{\mathbf{r}}'_1) \mathcal{P}_{L'_{20}}(R'\hat{\mathbf{r}}'_0, R'\hat{\mathbf{r}}'_2) \mathcal{P}_{L_3, L_{3s}, L'_3}(R\hat{\mathbf{r}}_3, -S\hat{\mathbf{s}}, -R'\hat{\mathbf{r}}'_3) \\ &= \sum_{\Lambda, \Lambda'} (-1)^{L_3} \overline{\mathcal{Q}}_{(\text{PC-P-S})}^{\Lambda, \Lambda'} \mathcal{P}_\Lambda(\hat{\mathbf{R}}) \mathcal{P}_{\Lambda'}(\hat{\mathbf{R}}'), \end{aligned} \quad (\text{C.16})$$

where we have defined:

$$\begin{aligned} \overline{\mathcal{Q}}_{(\text{PC-P-S})}^{\Lambda, \Lambda'} &\equiv \sum_{\text{All M}} c_M^\Lambda c_{M'}^{\Lambda'} D_{L_{10}} D_{L_{20}} D_{L'_{10}} D_{L'_{20}} D_{L_3} \\ &\times (-1)^{L_3} \sum_{L_0, M_0} G_{M_{10}, M_{20}, -M_0}^{L_{10}, L_{20}, L_0} \sum_{L'_0, M'_0} G_{M'_{10}, M'_{20}, -M'_0}^{L'_{10}, L'_{20}, L'_0}. \end{aligned} \quad (\text{C.17})$$

### C.5 $\widehat{\mathbf{s}}$ Integral for the PC-Half-Half Configuration

We conclude our analysis of the  $\widehat{\mathbf{s}}$  integrals by evaluating the PC-half-half configurations:

$$\begin{aligned} &\int dR dR' dS \mathcal{P}_{L_{10}}(R\widehat{\mathbf{r}}_0, R\widehat{\mathbf{r}}_1) \mathcal{P}_{L'_{10}}(R'\widehat{\mathbf{r}}'_0, R'\widehat{\mathbf{r}}'_1) \mathcal{P}_{L_{q20}, L_{q2s}, L'_{q20}}(R\widehat{\mathbf{r}}_0, -S\widehat{\mathbf{s}}, -R'\widehat{\mathbf{r}}'_0) \\ &\times \mathcal{P}_{L_2, L_{2s}, L'_2}(R\widehat{\mathbf{r}}_2, -S\widehat{\mathbf{s}}, -R'\widehat{\mathbf{r}}'_2) \mathcal{P}_{L_3, L_{3s}, L'_3}(R\widehat{\mathbf{r}}_3, -S\widehat{\mathbf{s}}, -R'\widehat{\mathbf{r}}'_3). \end{aligned} \quad (\text{C.18})$$

Expressing the 3-argument isotropic basis function in terms of the spherical harmonics we find the  $dS$  integral as:

$$\int dS Y_{L_{q2s}, M_{q2s}}(\widehat{\mathbf{s}}) Y_{L_{2s}, M_{2s}}(\widehat{\mathbf{s}}) Y_{L_{3s}, M_{3s}}(\widehat{\mathbf{s}}) = G_{M_{q2s}, M_{2s}, M_{3s}}^{L_{q2s}, L_{2s}, L_{3s}}. \quad (\text{C.19})$$

Then, the primed integrals can be evaluated to obtain:

$$\begin{aligned} &\int dR' Y_{L'_{10}, M'_{10}}(R'\widehat{\mathbf{r}}'_0) Y_{L'_{q20}, M'_{q20}}(R'\widehat{\mathbf{r}}'_0) Y_{L'_{10}, M'_{10}}(R'\widehat{\mathbf{r}}'_1) Y_{L'_2, M'_2}(R'\widehat{\mathbf{r}}'_2) Y_{L'_3, M'_3}(R'\widehat{\mathbf{r}}'_3) \\ &= \sum_{L'_0, M'_0} G_{M'_{10}, M'_{q20}, -M'_0}^{L'_{10}, L'_{q20}, L'_0} \int dR Y_{L'_0, M'_0}(R\widehat{\mathbf{r}}_0) Y_{L'_{10}, M'_{10}}(R\widehat{\mathbf{r}}_1) Y_{L'_2, M'_2}(R\widehat{\mathbf{r}}_2) Y_{L'_3, M'_3}(R\widehat{\mathbf{r}}_3) \\ &= \sum_{\Lambda'} c_{M'}^{\Lambda'} \mathcal{P}_{\Lambda'}(\widehat{\mathbf{r}}'_0, \widehat{\mathbf{r}}'_1, \widehat{\mathbf{r}}'_2, \widehat{\mathbf{r}}'_3) \sum_{L'_0, M'_0} G_{M'_{10}, M'_{q20}, -M'_0}^{L'_{10}, L'_{q20}, L'_0}, \end{aligned} \quad (\text{C.20})$$

where we have defined  $\Lambda' \equiv \{L'_0, L'_{10}, L'_2, L'_3\}$ . Following the same steps, we evaluate the unprimed integrals and find:

$$\begin{aligned} &\int dR Y_{L_{10}, M_{10}}(R\widehat{\mathbf{r}}_0) Y_{L_{q20}, M_{q20}}(R\widehat{\mathbf{r}}_0) Y_{L_{10}, M_{10}}(R\widehat{\mathbf{r}}_1) Y_{L_2, M_2}(R\widehat{\mathbf{r}}_2) Y_{L_3, M_3}(R\widehat{\mathbf{r}}_3) \\ &= \sum_{\Lambda} c_M^\Lambda \mathcal{P}_{\Lambda}(\widehat{\mathbf{r}}_0, \widehat{\mathbf{r}}_1, \widehat{\mathbf{r}}_2, \widehat{\mathbf{r}}_3) \sum_{L_0, M_0} G_{M_{10}, M_{q20}, -M_0}^{L_{10}, L_{q20}, L_0}, \end{aligned} \quad (\text{C.21})$$

where we have defined  $\Lambda \equiv \{L_0, L_{10}, L_2, L_3\}$ . Therefore, the result of evaluating the  $\widehat{\mathbf{s}}$  by means of averaging over all rotations results in:

$$\begin{aligned} &\int dR dR' dS \mathcal{P}_{L_{10}}(R\widehat{\mathbf{r}}_0, R\widehat{\mathbf{r}}_1) \mathcal{P}_{L'_{10}}(R'\widehat{\mathbf{r}}'_0, R'\widehat{\mathbf{r}}'_1) \mathcal{P}_{L_{q20}, L_{q2s}, L'_{q20}}(R\widehat{\mathbf{r}}_0, -S\widehat{\mathbf{s}}, -R'\widehat{\mathbf{r}}'_0) \\ &\times \mathcal{P}_{L_2, L_{2s}, L'_2}(R\widehat{\mathbf{r}}_2, -S\widehat{\mathbf{s}}, -R'\widehat{\mathbf{r}}'_2) \mathcal{P}_{L_3, L_{3s}, L'_3}(R\widehat{\mathbf{r}}_3, -S\widehat{\mathbf{s}}, -R'\widehat{\mathbf{r}}'_3) \\ &= \sum_{\Lambda, \Lambda_s, \Lambda'} \overline{\mathcal{Q}}_{(\text{PC-H-H})}^{\Lambda, \Lambda_s, \Lambda'} \mathcal{P}_{\Lambda}(\widehat{\mathbf{R}}) \mathcal{P}_{\Lambda'}(\widehat{\mathbf{R}}'), \end{aligned} \quad (\text{C.22})$$

where we have defined:

$$\begin{aligned} \overline{\mathcal{Q}}_{(\text{PC-H-H})}^{\Lambda, \Lambda_s, \Lambda'} &\equiv \sum_{\text{All M}} c_M^\Lambda c_{M'}^{\Lambda'} c_{M_{q20}, M_{q2s}, M'_{q20}}^{L_{q20}, L_{q2s}, L'_{q20}} c_{M_2, M_{2s}, M'_2}^{L_2, L_{2s}, L'_2} c_{M_3, M_{3s}, M'_3}^{L_3, L_{3s}, L'_3} \\ &\times D_{L_{10}} D_{L'_{10}} \sum_{L_0, M_0} G_{M_{10}, M_{q20}, -M_0}^{L_{10}, L_{q20}, L_0} \sum_{L'_0, M'_0} G_{M'_{10}, M'_{q20}, -M'_0}^{L'_{10}, L'_{q20}, L'_0}. \end{aligned} \quad (\text{C.23})$$

## D Splitting Products of Mixed-Space 2-Argument Isotropic Basis Functions

The PWE for a complex exponential of two arguments can be written in the isotropic basis as:

$$e^{-i\mathbf{k}\cdot(\mathbf{r}-\mathbf{x})} = (4\pi)^2 \sum_{\ell_r, \ell_x} i^{\ell_x - \ell_r} (-1)^{\ell_x + \ell_r} s_{\ell_r}^{(I)} s_{\ell_x}^{(I)} j_{\ell_r}(kr) j_{\ell_x}(kx) \mathcal{P}_{\ell_r}(\hat{\mathbf{k}}, \hat{\mathbf{r}}) \mathcal{P}_{\ell_x}(\hat{\mathbf{k}}, \hat{\mathbf{x}}), \quad (\text{D.1})$$

where we have two isotropic basis functions with mixed-space arguments<sup>7</sup>. The goal of this section is to separate these mixed-space isotropic functions into a product of isotropic functions of one space each (Fourier or position) as follows:

$$\mathcal{P}_{\ell_r}(\hat{\mathbf{k}}, \hat{\mathbf{r}}) \mathcal{P}_{\ell_x}(\hat{\mathbf{k}}, \hat{\mathbf{x}}) = \sum_{\ell_k} \delta_{\ell_r, \ell_x}^{\text{K}} \omega_{\ell_x, \ell_k} \mathcal{P}_{\ell_k}(\hat{\mathbf{k}}, \hat{\mathbf{k}}) \mathcal{P}_{\ell_x}(\hat{\mathbf{r}}, \hat{\mathbf{x}}). \quad (\text{D.2})$$

To prove this, we start by expressing the product of the two mixed-space isotropic basis function with a general form:

$$\mathcal{P}_{\ell_r}(\hat{\mathbf{k}}, \hat{\mathbf{r}}) \mathcal{P}_{\ell_x}(\hat{\mathbf{k}}, \hat{\mathbf{x}}) = \sum_{\ell_1, \ell_2} \bar{\omega}_{\ell_1, \ell_2} \mathcal{P}_{\ell_1}(\hat{\mathbf{k}}, \hat{\mathbf{k}}) \mathcal{P}_{\ell_2}(\hat{\mathbf{r}}, \hat{\mathbf{x}}). \quad (\text{D.3})$$

Multiplying both sides by the complex conjugate of the isotropic basis functions that we have on the right-hand side, we obtain:

$$\begin{aligned} \bar{\omega}_{\ell_1, \ell_2} &= \int \mathcal{P}_{\ell_r}(\hat{\mathbf{k}}, \hat{\mathbf{r}}) \mathcal{P}_{\ell_x}(\hat{\mathbf{k}}, \hat{\mathbf{x}}) \mathcal{P}_{\ell_1}^*(\hat{\mathbf{k}}, \hat{\mathbf{k}}) \mathcal{P}_{\ell_2}^*(\hat{\mathbf{r}}, \hat{\mathbf{x}}) \\ &= \frac{(-1)^{\ell_r + \ell_x + \ell_1 + \ell_2}}{s_{\ell_r}^{(I)} s_{\ell_x}^{(I)} s_{\ell_1}^{(I)} s_{\ell_2}^{(I)}} \sum_{m_r, m_x, m_1, m_2} \int Y_{\ell_r, m_r}(\hat{\mathbf{r}}) Y_{\ell_2, m_2}(\hat{\mathbf{r}}) \int Y_{\ell_x, m_x}(\hat{\mathbf{x}}) Y_{\ell_2, m_2}(\hat{\mathbf{x}}) \\ &\quad \times \int Y_{\ell_r, m_r}(\hat{\mathbf{k}}) Y_{\ell_x, m_x}(\hat{\mathbf{k}}) Y_{\ell_1, m_1}(\hat{\mathbf{k}}) Y_{\ell_1, m_1}^*(\hat{\mathbf{k}}) \\ &= \frac{(-1)^{\ell_x + \ell_1 + m_x + m_1}}{(s_{\ell_x}^{(I)})^3 s_{\ell_1}^{(I)}} \delta_{\ell_r, \ell_x}^{\text{K}} \sum_{\ell', m', m_1} G_{m_x, m_x, -m'}^{\ell_x, \ell_x, \ell'} G_{m', m_1, -m_1}^{\ell', \ell_1, \ell_1}, \end{aligned} \quad (\text{D.4})$$

where in the second equality, we expanded the isotropic basis functions into spherical harmonics, and in the third equality we have computed the angular integrals. We also defined:

$$s_{\ell_1}^{(I)} = \sqrt{2\ell + 1}, \quad (\text{D.5})$$

and the PWE can thus be written as:

$$e^{-i\mathbf{k}\cdot(\mathbf{r}-\mathbf{x})} = (4\pi)^2 \sum_{\ell_x, \ell_k} \omega_{\ell_x, \ell_k} j_{\ell_x}(kr) j_{\ell_x}(kx) \mathcal{P}_{\ell_k}(\hat{\mathbf{k}}, \hat{\mathbf{k}}) \mathcal{P}_{\ell_x}(\hat{\mathbf{r}}, \hat{\mathbf{x}}), \quad (\text{D.6})$$

where we have defined  $\omega$  as:

$$\omega_{\ell_1, \ell_2} = (2\ell_1 + 1) \bar{\omega}_{\ell_1, \ell_2} \equiv \left(s_{\ell_1}^{(I)}\right)^2 \bar{\omega}_{\ell_1, \ell_2}. \quad (\text{D.7})$$

---

<sup>7</sup>we mean the mixing of any wave-vectors  $\mathbf{k}$  with vectors  $\mathbf{r}$  within the arguments of the isotropic basis functions.

## E Forming the Connected 4PCF Covariance

We show how to form the connected 4PCF covariance terms entering at 1-loop. Following [15], every integral over correlation functions scales as  $r_c^3/V$ , where  $r_c \approx 100$  Mpc/h is the correlation length and  $V$  is the volume of the survey. The survey size tends to be much larger than the correlation length, hence for every integral involving a correlation function, we have a suppression of the order of  $(r_c^3/V)^\alpha$ , where  $\alpha = \{1, 2, 3, \dots\}$  indicates the number of integrals over correlation functions we have.

Therefore, we compute the connected 4PCF covariance with only the terms that are of the same order in  $r_c^3/V$ . We first define the components that give rise to the connected 4PCF, starting with the full 4PCF:

$$\hat{\zeta}^{(\text{full})}(\mathbf{r}_1, \mathbf{r}_2, \mathbf{r}_3) = \frac{1}{V} \int d\mathbf{x} \delta(\mathbf{x} + \mathbf{r}_0) \delta(\mathbf{x} + \mathbf{r}_1) \delta(\mathbf{x} + \mathbf{r}_2) \delta(\mathbf{x} + \mathbf{r}_3), \quad (\text{E.1})$$

following with the disconnected piece:

$$\hat{\zeta}^{(\text{disc.})}(\mathbf{r}_1, \mathbf{r}_2, \mathbf{r}_3) = \frac{1}{V} \int d\mathbf{x}_1 \delta(\mathbf{x}_1 + \mathbf{r}_0) \delta(\mathbf{x}_1 + \mathbf{r}_1) \frac{1}{V} \int d\mathbf{x}_2 \delta(\mathbf{x}_2 + \mathbf{r}_2) \delta(\mathbf{x}_2 + \mathbf{r}_3). \quad (\text{E.2})$$

Given the above definitions, to compute the connected 4PCF covariance we must then obtain:

$$\text{Cov}_{4,1\text{L}}^{[2],(c,c)} = \text{Cov}_{4,1\text{L}}^{[2],(\text{full},\text{full})} - \text{Cov}_{4,1\text{L}}^{[2],(\text{full},\text{disc})} - \text{Cov}_{4,1\text{L}}^{[2],(\text{disc},\text{full})} + \text{Cov}_{4,1\text{L}}^{[2],(\text{disc},\text{disc})}. \quad (\text{E.3})$$

We show how to calculate  $\text{Cov}^{(\text{full},\text{full})}$  with the second-order density contrast, but the other terms follow the same procedure:

$$\begin{aligned} \text{Cov}_{4,1\text{L}}^{[2],(\text{full},\text{full})} &= \left\langle \frac{1}{V} \int d\mathbf{x} \delta^{(2)}(\mathbf{x} + \mathbf{r}_0) \delta_{\text{lin.}}(\mathbf{x} + \mathbf{r}_1) \delta_{\text{lin.}}(\mathbf{x} + \mathbf{r}_2) \delta_{\text{lin.}}(\mathbf{x} + \mathbf{r}_3) \right. \\ &\quad \times \left. \frac{1}{V} \int d\mathbf{x}' \delta^{(2)}(\mathbf{x}' + \mathbf{r}_0') \delta_{\text{lin.}}(\mathbf{x}' + \mathbf{r}_1') \delta_{\text{lin.}}(\mathbf{x}' + \mathbf{r}_2') \delta_{\text{lin.}}(\mathbf{x}' + \mathbf{r}_3') \right\rangle. \end{aligned} \quad (\text{E.4})$$

We expand the second-order densities in terms of two linear densities in real space<sup>8</sup> and apply Wick's theorem to obtain:

$$\begin{aligned} \text{Cov}_{4,1\text{L}}^{[2],(\text{full},\text{full})} &\supset \frac{1}{V^2} \int d\mathbf{q}_1 d\mathbf{q}_2 \int d\mathbf{q}_1' d\mathbf{q}_2' \int d\mathbf{x} \int d\mathbf{x}' [\{ \langle \delta_{\text{lin.}}(\mathbf{x} + \mathbf{r}_0 + \mathbf{q}_1) \delta_{\text{lin.}}(\mathbf{x}' + \mathbf{r}_0' + \mathbf{q}_1') \rangle \\ &\quad \times \langle \delta_{\text{lin.}}(\mathbf{x} + \mathbf{r}_0 + \mathbf{q}_2) \delta_{\text{lin.}}(\mathbf{x}' + \mathbf{r}_0' + \mathbf{q}_2') \rangle \langle \delta_{\text{lin.}}(\mathbf{x} + \mathbf{r}_1) \delta_{\text{lin.}}(\mathbf{x}' + \mathbf{r}_1') \rangle \\ &\quad \times \langle \delta_{\text{lin.}}(\mathbf{x} + \mathbf{r}_2) \delta_{\text{lin.}}(\mathbf{x}' + \mathbf{r}_2') \rangle \langle \delta_{\text{lin.}}(\mathbf{x} + \mathbf{r}_3) \delta_{\text{lin.}}(\mathbf{x}' + \mathbf{r}_3') \rangle + 137 \text{ perms.}^9 \} \\ &\quad + \{ \langle \delta_{\text{lin.}}(\mathbf{x} + \mathbf{r}_0 + \mathbf{q}_1) \delta_{\text{lin.}}(\mathbf{x} + \mathbf{r}_1) \rangle \langle \delta_{\text{lin.}}(\mathbf{x} + \mathbf{r}_0 + \mathbf{q}_2) \delta_{\text{lin.}}(\mathbf{x}' + \mathbf{r}_0' + \mathbf{q}_2') \rangle \\ &\quad \times \langle \delta_{\text{lin.}}(\mathbf{x}' + \mathbf{q}_1' + \mathbf{r}_0') \delta_{\text{lin.}}(\mathbf{x}' + \mathbf{r}_1') \rangle \langle \delta_{\text{lin.}}(\mathbf{x} + \mathbf{r}_2) \delta_{\text{lin.}}(\mathbf{x}' + \mathbf{r}_2') \rangle \\ &\quad \times \langle \delta_{\text{lin.}}(\mathbf{x} + \mathbf{r}_3) \delta_{\text{lin.}}(\mathbf{x}' + \mathbf{r}_3') \rangle + 419 \text{ perms.}^{10} \} ] \\ &= \frac{1}{V} \int d\mathbf{q}_1 d\mathbf{q}_2 \int d\mathbf{q}_1' d\mathbf{q}_2' \int ds \\ &\quad \times [\{ \xi_W(\mathbf{r}_0 - \mathbf{s} - \mathbf{r}_0' + \mathbf{q}_1 - \mathbf{q}_1') \xi_W(\mathbf{r}_0 - \mathbf{s} - \mathbf{r}_0' + \mathbf{q}_2 - \mathbf{q}_2') \\ &\quad \times \xi(\mathbf{r}_1 - \mathbf{s} - \mathbf{r}_1') \xi(\mathbf{r}_2 - \mathbf{s} - \mathbf{r}_2') \xi(\mathbf{r}_3 - \mathbf{s} - \mathbf{r}_3') + 119 \text{ perms.} \} \\ &\quad + \{ \xi_W(\mathbf{r}_0 - \mathbf{r}_1 + \mathbf{q}_1) \xi_W(\mathbf{r}_0 - \mathbf{s} - \mathbf{r}_0' + \mathbf{q}_2 - \mathbf{q}_2') \xi_W(\mathbf{r}_0' - \mathbf{r}_1' + \mathbf{q}_1') \\ &\quad \times \xi(\mathbf{r}_2 - \mathbf{s} - \mathbf{r}_2') \xi(\mathbf{r}_3 - \mathbf{s} - \mathbf{r}_3') + 419 \text{ perms.} \} ], \end{aligned} \quad (\text{E.5})$$

<sup>8</sup>We set the second-order kernel to one just for the demonstration of how to construct the connected 4PCF covariance. In the main text, we evaluate the covariance with the second-order kernel incorporated.

where we express the correlation function derived from the second-order densities as  $\xi_W$  to express that this must actually be evaluated with their respective second-order kernel as shown in the main text. The resulting correlation functions in the last two lines arise from contracting density contrast within the same tetrahedron; we term these structures partially-connected correlations. All the above permutations are of the order  $\mathcal{O}(r_c^3/V)$ . Because of Eq. (E.3) all the terms with the same order,  $\mathcal{O}(r_c^3/V)$ , will cancel each other; terms that are suppressed in the full  $\times$  disconnected, disconnected  $\times$  full, and disconnected  $\times$  disconnected pieces will not cancel the full  $\times$  full piece. This means we must check the full  $\times$  disconnected, disconnected  $\times$  full, and disconnected  $\times$  disconnected pieces carefully to determine which terms enter the connected 4PCF covariance at the 1-loop level. We find that only the two partially-connected configurations depicted in Figure 4 enter the covariance. Below, we show an example of one of the partially-connected permutations that is being suppressed in the full  $\times$  disconnected, disconnected  $\times$  full, and disconnected  $\times$  disconnected pieces, hence entering the covariance:

$$\begin{aligned}
\text{Cov}_{4,1L}^{[2],(\text{full},\text{disc.})} &\supset \frac{1}{V^3} \int d\mathbf{q}_1 d\mathbf{q}_2 \int d\mathbf{q}'_1 d\mathbf{q}'_2 \int d\mathbf{x} \int d\mathbf{x}'_1 \int d\mathbf{x}'_2 \\
&\times [\langle \delta_{\text{lin.}}(\mathbf{x} + \mathbf{r}_0 + \mathbf{q}_1) \delta_{\text{lin.}}(\mathbf{x} + \mathbf{r}_1) \rangle \langle \delta_{\text{lin.}}(\mathbf{x} + \mathbf{r}_0 + \mathbf{q}_2) \delta_{\text{lin.}}(\mathbf{x}'_1 + \mathbf{r}'_0 + \mathbf{q}'_2) \rangle \\
&\langle \delta_{\text{lin.}}(\mathbf{x}'_1 + \mathbf{q}'_1 + \mathbf{r}'_0) \delta_{\text{lin.}}(\mathbf{x}'_1 + \mathbf{r}'_1) \rangle \langle \delta_{\text{lin.}}(\mathbf{x} + \mathbf{r}_2) \delta_{\text{lin.}}(\mathbf{x}'_2 + \mathbf{r}'_2) \rangle \\
&\times \langle \delta_{\text{lin.}}(\mathbf{x} + \mathbf{r}_3) \delta_{\text{lin.}}(\mathbf{x}'_2 + \mathbf{r}'_3) \rangle + 71 \text{ perms.}^{11}] \\
&= \frac{1}{V^2} \int d\mathbf{q}_1 d\mathbf{q}_2 \int d\mathbf{q}'_1 d\mathbf{q}'_2 \int d\mathbf{s} \int d\mathbf{s}' \\
&\times [\xi_W(\mathbf{r}_0 - \mathbf{r}_1 + \mathbf{q}_1) \xi_W(\mathbf{r}_0 - \mathbf{s} - \mathbf{r}'_0 + \mathbf{q}_2 - \mathbf{q}'_2) \\
&\times \xi_W(\mathbf{r}'_0 - \mathbf{r}'_1 + \mathbf{q}'_1) \xi(\mathbf{r}_2 - \mathbf{s}' - \mathbf{r}'_2) \xi(\mathbf{r}_3 - \mathbf{s}' - \mathbf{r}'_3) + 71 \text{ perms.}] , \tag{E.6}
\end{aligned}$$

where we defined  $\mathbf{s} = \mathbf{x} - \mathbf{x}'_1$  and  $\mathbf{s}' = \mathbf{x} - \mathbf{x}'_2$ . The above result gets suppressed by  $r_c^6/V^2$ .

Calculating disconnected  $\times$  full term of the covariance follows the same procedure, and results in the same number of permutations being suppressed:

$$\begin{aligned}
\text{Cov}_{4,1L}^{[2],(\text{disc.},\text{disc.})} &\supset \frac{1}{V^4} \int d\mathbf{q}_1 d\mathbf{q}_2 \int d\mathbf{q}'_1 d\mathbf{q}'_2 \int d\mathbf{x}_1 \int d\mathbf{x}_2 \int d\mathbf{x}'_1 \int d\mathbf{x}'_2 \\
&\times [\langle \delta_{\text{lin.}}(\mathbf{x}_1 + \mathbf{r}_0 + \mathbf{q}_1) \delta_{\text{lin.}}(\mathbf{x}_1 + \mathbf{r}_1) \rangle \langle \delta_{\text{lin.}}(\mathbf{x}_1 + \mathbf{r}_0 + \mathbf{q}_2) \delta_{\text{lin.}}(\mathbf{x}'_1 + \mathbf{r}'_0 + \mathbf{q}'_2) \rangle \\
&\times \langle \delta_{\text{lin.}}(\mathbf{x}'_1 + \mathbf{q}'_1 + \mathbf{r}'_0) \delta_{\text{lin.}}(\mathbf{x}'_1 + \mathbf{r}'_1) \rangle \langle \delta_{\text{lin.}}(\mathbf{x}_2 + \mathbf{r}_2) \delta_{\text{lin.}}(\mathbf{x}'_2 + \mathbf{r}'_2) \rangle \\
&\times \langle \delta_{\text{lin.}}(\mathbf{x}_2 + \mathbf{r}_3) \delta_{\text{lin.}}(\mathbf{x}'_2 + \mathbf{r}'_3) \rangle + 71 \text{ perms.}] \\
&= \frac{1}{V^2} \int d\mathbf{q}_1 d\mathbf{q}_2 \int d\mathbf{q}'_1 d\mathbf{q}'_2 \int d\mathbf{s}_1 \int d\mathbf{s}'_2 \\
&\times [\xi_W(\mathbf{r}_0 - \mathbf{r}_1 + \mathbf{q}_1) \xi_W(\mathbf{r}_0 - \mathbf{s}_1 - \mathbf{r}'_0 + \mathbf{q}_2 - \mathbf{q}'_2) \\
&\times \xi_W(\mathbf{r}'_0 - \mathbf{r}'_1 + \mathbf{q}'_1) \xi(\mathbf{r}_2 - \mathbf{s}'_2 - \mathbf{r}'_2) \xi(\mathbf{r}_3 - \mathbf{s}'_2 - \mathbf{r}'_3) + 71 \text{ perms.}] , \tag{E.7}
\end{aligned}$$

<sup>10</sup>Number of permutation has been obtained by adding the permutations counted in the main text for the fully-coupled terms.

<sup>10</sup>Finding the number of permutations is done in three steps. i) Choose one of the second-order densities in either of the two tetrahedra, then pair this second-order density with any of the densities from the same tetrahedron; one has 4 possibilities. ii) Pair the remaining second-order density with any density in any of the two tetrahedrons; one has 7 possibilities. iii) Repeat with the opposite tetrahedron; one has 15 possibilities. Total number of permutations =  $4 \times 7 \times 15 = 420$  perms.

<sup>11</sup>Number of permutation has been obtained by adding the permutations counted in the main text for the partially-coupled terms.

where we defined  $\mathbf{s}_1 = \mathbf{x}_1 - \mathbf{x}'_1$  and  $\mathbf{s}'_2 = \mathbf{x}_2 - \mathbf{x}'_2$ . This term is also suppressed at  $\mathcal{O}(r_c^3/V)$ . As anticipated, all of the partially-connected terms at order of  $\mathcal{O}(r_c^3/V)$  will cancel out in Eq. (E.3), while those terms that are being suppressed will not cancel out and hence need to be accounted for when computing the connected 4PCF covariance. Below we show an example of the terms that one needs to account for:

$$\begin{aligned} \text{Cov}_{4,1L}^{[2],(c,c)} = \frac{1}{V} \int d\mathbf{q}_1 d\mathbf{q}_2 \int d\mathbf{q}'_1 d\mathbf{q}'_2 \int d\mathbf{s} [ & \{ \xi_W(\mathbf{r}_0 - \mathbf{s} - \mathbf{r}'_0 + \mathbf{q}_1 - \mathbf{q}'_1) \xi_W(\mathbf{r}_0 - \mathbf{s} - \mathbf{r}'_0 + \mathbf{q}_2 - \mathbf{q}'_2) \\ & \times \xi(\mathbf{r}_1 - \mathbf{s} - \mathbf{r}'_1) \xi(\mathbf{r}_2 - \mathbf{s} - \mathbf{r}'_2) \xi(\mathbf{r}_3 - \mathbf{s} - \mathbf{r}'_3) + 119 \text{ perms.} \} \\ & + \{ \xi_W(\mathbf{r}_0 - \mathbf{r}_1 + \mathbf{q}_1) \xi_W(\mathbf{r}_0 - \mathbf{s} - \mathbf{r}'_0 + \mathbf{q}_2 - \mathbf{q}'_2) \xi_W(\mathbf{r}'_0 - \mathbf{r}'_1 + \mathbf{q}'_1) \\ & \times \xi(\mathbf{r}_2 - \mathbf{s} - \mathbf{r}'_2) \xi(\mathbf{r}_3 - \mathbf{s} - \mathbf{r}'_3) + 71 \text{ perms.} \} ] . \end{aligned} \quad (\text{E.8})$$

## References

- [1] Bernardeau F., et al., "Large-scale structure of the universe and cosmological perturbation theory," *Physics Reports*, Sept. 2002.
- [2] Bertolini D., et al., "Non-Gaussian covariance of the matter power spectrum in the effective field theory of large scale structure," *PRD*, June 2016.
- [3] Cahn R. N., Slepian Z., "Isotropic N-point basis functions and their properties," *J. Phys. A Math. Gen.*, Aug. 2023.
- [4] Cahn R. N., Slepian Z., Hou J., "Test for Cosmological Parity Violation Using the 3D Distribution of Galaxies," *PRL*, Volume 130, Issue 20, article id.201002, May 2023.
- [5] Chellino J., Slepian Z., "Triple-spherical Bessel function integrals with exponential and Gaussian damping: towards an analytic N-point correlation function covariance model," *PRSA*, Vol. 479, Issue 2276, Art. id.20230138, Aug. 2023.
- [6] DESI Collaboration, et al., "DESI 2024 V: Full-Shape Galaxy Clustering from Galaxies and Quasars," *arXiv e-prints* 2411.12021, Nov. 2024.
- [7] DLMF, NIST Digital Library of Mathematical Functions. <http://dlmf.nist.gov/>
- [8] Hou J., et al., "Analytic Gaussian covariance matrices for galaxy N-point correlation functions," *PRD*, Aug. 2022.
- [9] Hou J., et al., "Measurement of parity-odd modes in the large-scale 4-point correlation function of Sloan Digital Sky Survey Baryon Oscillation Spectroscopic Survey twelfth data release CMASS and LOWZ galaxies," *MNRAS*, May 2023.
- [10] Hou J., et al., "Study of the Connected Four-Point Correlation Function of Galaxies from DESI Data Release 1 Luminous Red Galaxy Sample," *arXiv:2508.09070*, Aug. 2025.
- [11] Kamalinejad F., Slepian Z., "A Non-Degenerate Neutrino Mass Signature in the Galaxy Bispectrum," *arXiv e-prints* 2011.00899, Nov. 2020.
- [12] Mohammed I., et al., "Perturbative approach to covariance matrix of the matter power spectrum," *MNRAS*, April 2017.
- [13] Ortola Leonard W., Slepian Z., Hou J., "A Model for the Redshift-Space Galaxy 4-Point Correlation Function," *arXiv e-prints* 2402.15510, Feb. 2024.
- [14] Ortola Leonard W., Slepian Z., "Analytical Template for the 4-Point Correlation Function Covariance Beyond the Gaussian Random Field II: 1-loop Corrections with Third-Order Densities," *In prep.*
- [15] Philcox, O.H.E., Hou J., Slepian Z., "A First Detection of the Connected 4-Point Correlation Function of Galaxies Using the BOSS CMASS Sample," *eprint arXiv:2108.01670*, Aug. 2021.

- [16] Philcox, O.H.E., "Probing parity violation with the four-point correlation function of BOSS galaxies," PRD, Sept. 2022.
- [17] Scoccimarro R., et al., "The Bispectrum as a Signature of Gravitational Instability in Redshift Space," AJ, June 1999.
- [18] Slepian Z., Chellino J., Greco A., "On a generating function for the isotropic basis functions and other connected results," Journal of Physics A: Mathematical and Theoretical, Volume 57, Issue 50, id.505203, 32 pp., Dec. 2024.
- [19] Slepian Z., Eisenstein D. J., "Modeling the large-scale redshift-space 3-point correlation function of galaxies," MNRAS, Volume 469, Issue 2, p.2059-2076, Aug. 2017.
- [20] Slepian Z., et al., "Measurement of Parity-Violating Modes of the Dark Energy Spectroscopic Instrument (DESI) Year 1 Luminous Red Galaxies' 4-Point Correlation Function," arXiv:2508.09133, Aug. 2025.
- [21] Wadekar D., Scoccimarro R., "Galaxy power spectrum multipoles covariance in perturbation theory," PRD, Dec. 2020.